Prediction model for hardened state properties of silica fume and fly ash based concrete incorporating silicomanganese slag

Matthew Zhi Yeon Ting, Kwong Soon Wong, Muhammad Ekhlasur Rahman, Selowara Joo Meheron

Abstract

Growing concrete consumption has gradually depleted conventional resources and the search for alternative sources is vital. The use of silicomanganese (SiMn) slag, industrial waste from smelting plant, for the substitution of limestone as concrete coarse aggregate, enhances sustainability. However, SiMn slag can reduce concrete strength and durability due to its lower abrasion resistance compared to limestone. The objective of this study is therefore to incorporate silica fume (SF) and fly ash (FA) in order to improve the strength and durability of SiMn slag concrete. To achieve the objective, prediction models for strength, durability and workability were developed using the Response Surface Method (RSM). The models were used for optimization to determine the optimum combination of SF and FA in the concrete. SF compensated for reduced concrete strength caused by FA at 7 days, and improved compressive and tensile strengths by 9.4% and 17.9% respectively at later age. The combination of SF and FA reduced sorptivity and chloride permeability by 20.3% and 62.5% at 180 days respectively. Prediction models expressed as polynomial functions of SF and FA have been developed based on experimental results. Analysis of variance (ANOVA) showed that the models were fit for prediction and optimization of concrete properties. Optimization and experimental validation indicated that a combination of 11.5% SF and 16.3% FA produced concrete that satisfied the optimization criteria. The models can also be used to predict the compressive strength of limestone concrete containing SF and FA by using an established linear equation with SiMn slag concrete.

Keywords: Prediction model, optimization, limestone, marine sand, seawater

27

1. Introduction

The use of industrial wastes as a substitute of concrete components is a promising strategy for concrete industry to implement economic and sustainability concepts. This study exploits the concepts by incorporating industrial wastes like silicomanganese (SiMn) slag, silica fume and fly ash into concrete. SiMn slag is a by-product of the smelting of silicon and manganese for alloy inclusion in steel production. The production of SiMn alloy generates about 1.2 times the SiMn slag from electric arc furnace, and this creates problems in waste management [1]. It is uncomplimentary for the smelting plant to store a large amount of waste due to uneconomical and space-demanding reasons. This waste is usually disposed of by landfill and sometimes used as road paving materials [2]. Nonetheless, SiMn slag has recently been substituted as materials for concrete production. Frias et al. [3] showed that cement replaced by grounded SiMn slag up to 15% could be used as supplementary cementitious material. Research on the use of granulated SiMn slag in Portland slag cement was also carried out by Nath and Kumar [4], who highlighted the pozzolanic property of SiMn slag. Allahverdi and Ahmadnezhad [5] confirmed that SiMn slag had mild pozzolanic property. The alkali activation of SiMn slag was also investigated by Navarro et al. [6]. However, the use of SiMn slag as coarse aggregate in concrete has rarely been studied. The other study performed by the authors [7] has shown that the use of SiMn slag as coarse aggregate reduced the compressive and tensile strengths of concrete as well as its durability at early age. An aim of this study is therefore to improve the strength and durability of SiMn slag concrete by using silica fume and fly ash.

A number of studies have explored the effect of silica fume (SF) and fly ash (FA) on concrete properties in order to determine their optimum replacement levels. Bhanja and Sengupta [8] found that the compressive and tensile strengths of concrete increased

53 with SF incorporation. Mazloom et al. [9] demonstrated that SF improved the
54 compressive strength and elastic modulus of concrete, but excess incorporation led to a
55 loss of concrete workability. Song et al. [10] showed that SF reduced permeability of
56 concrete. As for the effect of FA, Kwan and Chen [11] discovered that the workability
57 of concrete improved with the addition of FA. Ponikiewski and Gołaszewski [12]
58 reported that FA led to lower concrete strength and durability at an early age, but
59 improved them at a later age. Sumer [13] also observed similar trends for class-F FA,
60 while the class-C FA showed better performance than the class-F FA at an early age.

61 The published literature also discussed the use of ternary blends of SF and FA in cement.
62 Radlinski and Olek [14] presented the result of the synergistic effect of SF and FA,
63 which considerably enhanced concrete strength and durability. Similarly, the research
64 performed by Bagheri et al. [15] showed an improvement in strength and durability,
65 particularly for concrete over 28 days of age. In the study of Erdem and Kırca [16], for
66 a constant SF content, the optimum replacement percentage of FA was between 10%
67 and 40%. Thomas et al. [17] found that the combination of 3–5% SF and 20–30% FA
68 produced concrete with better resistance against alkali-silica reaction and sulphate
69 attack. Although numerous studies have been conducted to investigate the effects of SF
70 and FA, the proportions of SF and FA yielding optimum concrete properties remains
71 unclear, especially in the ternary system. The findings differ from literature to literature
72 due to variations in material properties and proportion of concrete mixture used. It is
73 therefore essential to study the effect of SF and FA as binary and ternary cement blends
74 in more details so that they can be used to enhance the properties of SiMn slag concrete.

75 An optimization method is required to determine the combination of SF and FA which
76 gives the best concrete properties. Statistical modelling is an optimization method that
77 relates decision variables to the design objective through mathematical configuration.

78 The established relationship enables the prediction of concrete properties and is useful
79 for optimizing the concrete mixture. This method has been used in several studies to
80 evaluate concrete properties. Nehdi and Summer [18] used the factorial experiment
81 method to optimize the SF and FA contents of ternary cement blend. However, the
82 analysis could not be considered to be conclusive due to the limited number of
83 experiments performed over a wide range of replacement level used. Muthukumar et al.
84 [19] carried out optimization of silica aggregates in polymer concrete using the Box-
85 Behnken design method. A total of 54 concrete mixtures of different design variable
86 combinations were used. The developed statistical model had a high correlation
87 coefficient of 0.96. Using the Response Surface Method (RSM), Güneyisi et al. [20]
88 found that the optimum combination of metakaolin and FA was 13% and 10%
89 respectively in terms of concrete durability. Rezaifar et al. [21] also used RSM for the
90 optimization of hybrid blends of crumb rubber and metakaolin. The developed
91 statistical model was experimentally verified to have an error below 10%. The literature
92 review shows that the statistical optimization approach can be used to study the binary
93 and ternary effects of FA and SF in this research.

94 Against this background, the aim of this research is to use the binary and ternary cement
95 blends of SF and FA for compensating the drawback of SiMn slag concrete in terms of
96 strength and durability. The study investigates the interactions between SF and FA in
97 SiMn slag concrete by statistically evaluating the experimental results. The
98 relationships are established between the replacement levels of SF and FA with
99 concrete strength, durability and workability. Prediction model of the concrete
100 properties is developed by using the Response Surface Method (RSM) for optimization.
101 The outcomes of optimization are also experimentally validated. Furthermore, the

prediction model is used to predict the properties of concrete produced from the limestone aggregate to demonstrate its applicability.

2. Research program

The objective of this research is to improve the SiMn slag concrete previously studied by Ting et al. [7]. The concrete was produced from cement as binder, SiMn slag as coarse aggregate, marine sand as fine aggregate and seawater. Similar concrete mix proportions have been used in this investigation, but with SF and FA as partial cement replacements.

2.1. Materials

The ordinary Portland cement (OPC) used was graded as CEM 1 42.5 N and complied with ASTM C150 standard [22]. FA and SF were incorporated to partially replace the OPC. Table 1 presents the chemical compositions of the FA and SF. Figure 1 shows the phase compositions of FA and SF which are consistent with the chemical compositions. The coarse aggregate used was silicomanganese (SiMn) slag. Limestone (LS) as coarse aggregate was also used for comparison purpose. As for the fine aggregate, the marine sand sampled at Tanjung Lobang Beach in Miri, Malaysia was used. Due to its high fineness, 30% of the sand volume was replaced by quarry dust. Table 2 presents the particle size distribution and physical properties of the coarse and fine aggregates. Seawater was used as mixing water and its chemical composition was tested and shown in Table 3. Sodium naphthalene sulphonate formaldehyde was used as the superplasticizer (SP) to enhance the concrete workability.

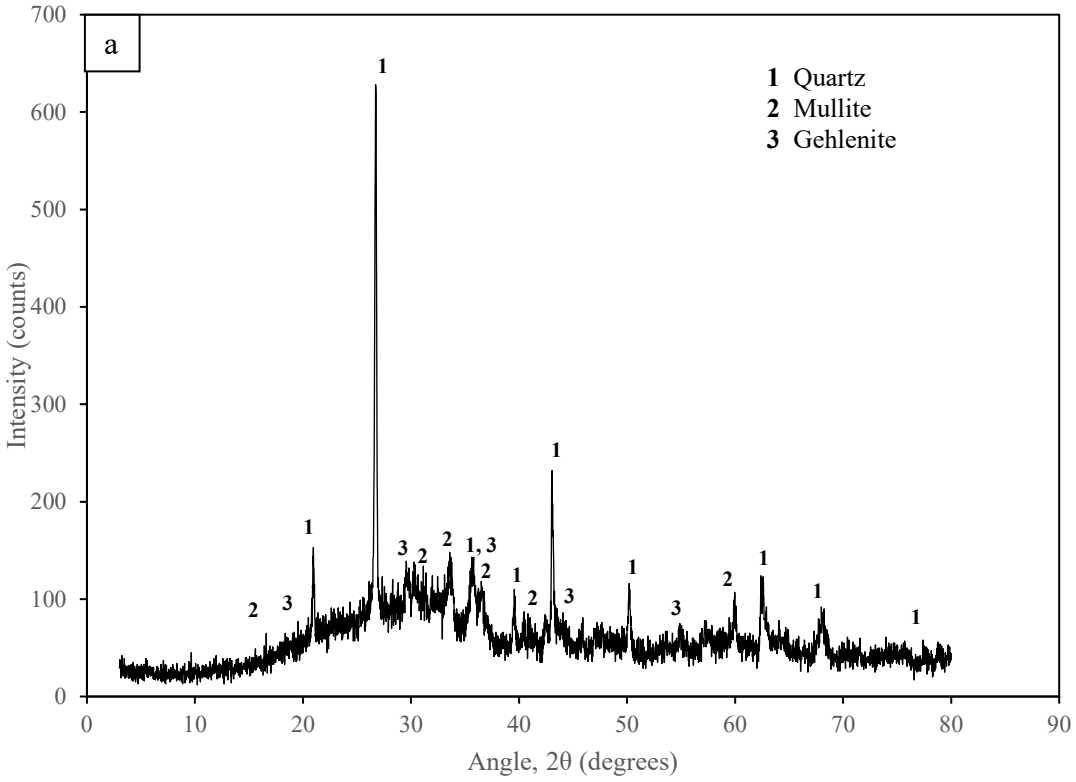

125

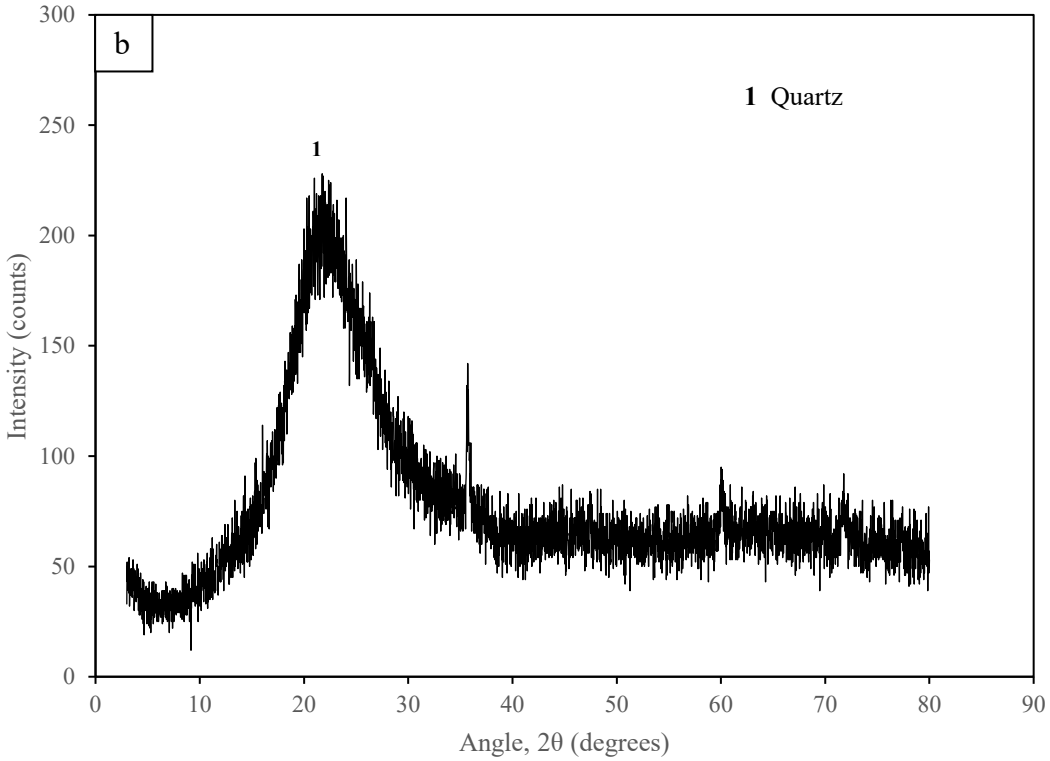

126

127 **Figure 1: XRD of (a) fly ash and (b) silica fume particles**

128 **Table 1: Chemical compositions of FA and SF**

	Specific gravity	Chemical compositions (%)								
		CaO	SiO_2	Al_2O_3	Fe_2O_3	MgO	SO_3	K_2O	Na_2O	L. O. I.
Fly ash	2.98	18.86	38.91	13.40	15.68	3.99	1.84	2.50	2.11	1.66
Silica fume	2.43	0.06	96.21	0.04	0.15	0.46	-	0.28	0.09	1.71

129

130 **Table 2: Sieve analysis and physical properties of aggregates**

Sieve size (mm)	Cumulative passing (%)		
	Marine sand mixture	SiMn slag	Limestone
37.5	-	100.0	-
25.0	-	33.7	100.0
19.0	-	28.2	92.6
12.5	-	8.5	87.5
9.5	-	4.8	32.8
4.75	100.0	0.0	12.1
2.36	95.1	-	0.0
1.18	80.7	-	-
0.6	70.9	-	-
0.3	31.7	-	-
0.15	3.2	-	-
0.075	0.0	-	-
Fineness modulus	3.18	9.25	6.75
Specific gravity	2.67	2.97	2.64
Abrasion resistance (%)	-	22	12
Water absorption (%)	-	0.21	0.66

131

132 **Table 3: Chemical constituents of seawater [7]**

Density	pH	Chemical compositions (mg/l)					
(26 ± 0.5 °C)	(26 ± 0.5 °C)	Na	Mg	Ca	K	Cl	SO_4
1.01 g/cm^3	8.1	17840	460	613	456	19675	1730

133 *2.2. Response Surface Method*

134 Response surface method (RSM) is a statistical technique used to develop a
135 mathematical model that describes one or more responses over a range of input
136 variables [23]. The RSM establishes a polynomial relationship between the responses
137 and the variables, including their influence and significance to the model. The model
138 can be used to predict and optimize the response. The development of the statistical
139 model begins with the collection of experimental data, followed by the selection of an
140 appropriate model to fit the data. The model is then evaluated for adequacy. A statistical
141 software, Design Expert v11, has been used for the design of experiment, mathematical
142 formulation, statistical analysis and response optimization [24]. This software uses
143 analysis of variance (ANOVA) to investigate the interaction among variables as well
144 as their influence on the response.

145 The responses studied in this investigation are compressive strength (y_1), splitting
146 tensile strength (y_2), sorptivity (y_3), chloride permeability (y_4) and slump value (y_5).
147 The variables that control these responses are FA/B (x_1) and SF/B (x_2), which represent
148 the ratio of fly ash and silica fume contents to the total binder, respectively. The variable
149 ranges are 0–0.4 for FA/B and 0–0.3 for SF/B. Ponikiewski and Gołaszewski [12]
150 recommended the use of FA up to 30%, while Kwan and Chen [11] suggested an
151 addition not exceeding 40%. This study therefore chooses the upper limit of 40% to
152 avoid excessive loss of concrete strength due to the FA replacement [13]. As for SF,
153 Aldahdooh et al. [25] and Tripathi et al. [26] found an optimum replacement level of
154 23% and 20% respectively. The SF replacement level used in this study is limited to
155 30% because further addition will increase concrete cohesiveness and affect the mixture
156 homogeneity [27].

The mathematical formulation developed using RSM can be expressed as a quadratic or higher-order polynomial equation as shown in Eq. (1).

$$y = \beta_o + \sum_{i=1}^{k} \beta_i x_i + \sum_{i=1}^{k} \beta_j {x_i}^2 + \sum_{i}^{k} \sum_{j}^{k} \beta_{ij} x_i x_j + \cdots + \sum_{i}^{k} \beta_h {x_h}^h + \varepsilon \quad (1)$$

In the equation, y denotes the response, x indicates the coded value of variable, β is the coefficient of regression, k is the number of variable, i, j as well as h are the polynomial degrees of the model representing linear, quadratic and higher-order polynomials respectively, and ε is a random error in the system [21, 28].

2.3. Design of concrete mixture

Table 4 shows twenty-two concrete mixtures used to assess the strength and durability of SF and FA based concrete. The Central Composite Design (CCD) method, an effective approach to design experiments, was used to develop these combinations of concrete mixtures. Two variables, FA/B and SF/B, were inputs for the design of experiment. Figure 2 illustrates all the design points of the CCD, where each point represents one type of concrete mixture. The variables at the boundary in CCD are coded as α. The face-centered CCD was used, which limited the coded values of +α and -α to +1 and -1 respectively. These coded values refer to the area bound by the regression model that is effective in predicting the response. This method initially recommended thirteen concrete mixtures, which were mix no. 1–4 as factorial points, 5–8 as axial points and 9–13 as center points as shown in Figure 2. Five center points were used to compute the error within concrete mixture and to determine the repeatability. However, the recommended concrete mixtures had a large gap between

178 the design points, which was not sufficient to produce a more precise trend in
179 experimental results. As such, eight additional concrete mixtures (mix no. 14–21)
180 distributed at the boundary of variables were included, as shown in Figure 2.

181 Control concrete mix design denoted as “Control” was obtained from the study carried
182 out by Ting et al. [7]. FA and SF were incorporated to partially replace the OPC of
183 Control mix in accordance with the outcome of CCD. The incorporation of FA and SF
184 was based on the absolute volume concept as shown in Table 4. Mix description was
185 used to denote the detail of binder replacement level of each mixture. For example, mix
186 no. 4 was referred to as “FA40SF30”, which indicated a ternary blend of 40% FA and
187 30% SF. The water-to-cement ratio of all mixtures remained constant at 0.32. The
188 dosage of superplasticizer (SP) was 1% of the total binder content. In order to study the
189 effect of FA and SF on concrete workability, the SP dosage remained constant. The
190 compaction time of fresh concrete would be increased if the workability was found to
191 be unsatisfactory in accordance with ASTM C192 standard [29]. This was to ensure the
192 homogeneity of the concrete produced. Compressive strength, splitting tensile strength,
193 sorptivity, chloride permeability and slump value of all mixtures were determined. Mix
194 no. 0 referred to as “Limestone” was included for comparison purpose. Limestone mix
195 had the same mixture proportions as Control mix, except that SiMn slag was completely
196 replaced by limestone as a coarse aggregate.

197

198 **Table 4: Proportions of concrete mixtures**

Mix no.	Mix description	FA/B	SF/B	OPC (kg/m^3)	SiMn slag (kg/m^3)	Marine sand (kg/m^3)	Quarry dust (kg/m^3)	Seawater (kg/m^3)	SP (kg/m^3)
0	Limestone	0	0	550	965*	515	173	176	5.5
1	Control	0	0	550	1115	515	173	176	5.5
2	SF30	0	0.3	385	1115	488	164	176	5.5
3	FA40	0.4	0	330	1115	508	171	176	5.5
4	FA40SF30	0.4	0.3	165	1115	481	161	176	5.5
5	FA20	0.2	0	440	1115	512	172	176	5.5
6	FA20SF30	0.2	0.3	275	1115	484	162	176	5.5
7	SF15	0	0.15	468	1115	501	168	176	5.5
8	FA40SF15	0.4	0.15	248	1115	494	166	176	5.5
9	FA20SF15	0.2	0.15	358	1115	498	167	176	5.5
10	FA20SF15	0.2	0.15	358	1115	498	167	176	5.5
11	FA20SF15	0.2	0.15	358	1115	498	167	176	5.5
12	FA20SF15	0.2	0.15	358	1115	498	167	176	5.5
13	FA20SF15	0.2	0.15	358	1115	498	167	176	5.5
14	SF7.5	0	0.075	509	1115	508	171	176	5.5
15	SF22.5	0	0.225	426	1115	495	166	176	5.5
16	FA10	0.1	0	495	1115	514	172	176	5.5
17	FA30	0.3	0	385	1115	510	171	176	5.5
18	FA10SF30	0.1	0.3	330	1115	486	163	176	5.5
19	FA30SF30	0.3	0.3	220	1115	482	162	176	5.5
20	FA40SF7.5	0.4	0.075	289	1115	501	168	176	5.5
21	FA40SF22.5	0.4	0.225	206	1115	488	164	176	5.5

FA/B is the ratio of fly ash content to the total binder content.

SF/B is the ratio of silica fume content to the total binder content.

*Limestone was used to fully replace the SiMn slag as coarse aggregate in this mixture.

199

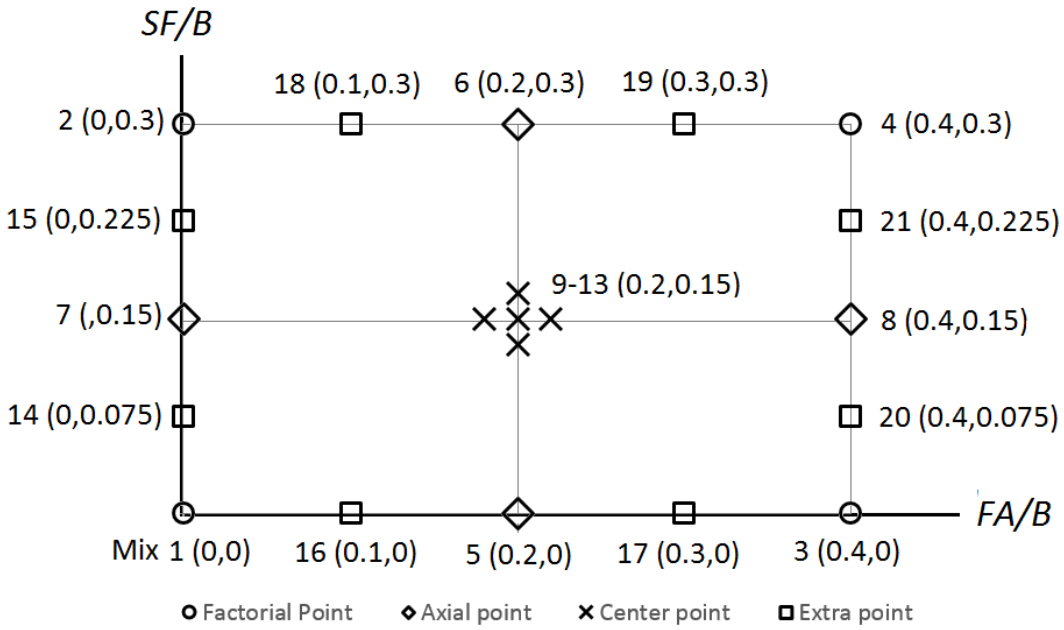

Figure 2: Design of experiment using CCD

2.4. Experimental methods

2.4.1. Preparation of concrete specimens

Concrete mixing was carried out using a 0.1m^3 capacity laboratory mixer with a mixing speed of 25 rpm. FA and SF were first blended with OPC before mixing with coarse and fine aggregates in order to ensure a uniform distribution of the binder. The total time for the concrete mixing was 3 to 5 minutes. The opening of the mixer was covered with a plastic sheet during the mixing process to avoid material loss. Concrete was casted into steel moulds in three layers and compacted using a vibrating table. The casted specimens were covered with a plastic sheet and placed in the curing room at 27±1 ºC for 1 day. The specimens were then removed from the moulds and cured by fully submerging them in water until the time of testing. Figure 3 depicts the stages for the preparation of concrete specimens and Figure 4 shows the testing of concrete specimens. Three replicates of concrete specimens were prepared and the average value

of each concrete property was used for analysis. The specimens of each concrete mixture were prepared from the same batch to reduce the test inconsistency. The workability of concrete was also determined by conducting the slump test in accordance with ASTM C143 [30].

Figure 3: Concrete specimens (a) mixing, (b) casting, (c) demoulding and (d) curing

2.4.2. Compressive strength test

The compression test was performed on cube specimens with dimensions of 100 x 100 x 100 mm using 3000kN compression testing machine. The test was performed in accordance with ASTM C39 standard [31]. Concrete specimens were tested after 7, 28 and 90 days of curing. In addition, the compressive strength of Control and Limestone mixes was determined at 1, 7, 14, 28, 56 and 90 days.

229 *2.4.3. Splitting tensile strength test*

230 The splitting tensile strength of concrete specimens was tested at 7, 28 and 90 days.
231 Cylindrical specimens of 100 x 200 mm were prepared and tested in accordance with
232 ASTM C496 standard [32].

233 *2.4.4. Sorptivity test*

234 The rate of water absorption of concrete, often referred to as sorptivity, was assessed
235 by carrying out uni-directional water absorption test. The test was conducted in
236 accordance with ASTM C1585 standard [33]. Cylindrical specimens of 100 x 50 mm
237 were trimmed from a 100 x 200 mm concrete cylinder using wet cutting method. The
238 specimens were dried in the oven at 50±1 ^{o}C for 7 days until a constant mass had been
239 reached. Side surfaces of the specimens were sealed with an epoxy coating. The test
240 started by placing the specimens on support rods in a plastic tray, exposing the unsealed
241 bottom surface to water. The water level was maintained at 2±1 mm during the test
242 period. Changes in the mass of specimens were recorded for 8 days. The sorptivity of
243 concrete was determined from the slope of water absorption curve against the square
244 root of time. The test was conducted on concrete specimens after 28, 90 and 180 days
245 of curing.

246 *2.4.5. Rapid chloride penetration test*

247 Concrete resistance to chloride penetration was assessed by the rapid chloride
248 penetration test (RCPT) in accordance with the standard procedure in ASTM C1202
249 [34]. Cylindrical specimens of 100 x 50 mm were prepared and tested for 28, 90 and
250 180 days. After standard conditioning, two faces of the specimen were attached to the
251 test cells, one face contacting 3% sodium chloride (NaCl) solution and the other face
252 touching 0.3 N sodium hydroxide (NaOH) solution. Electrical current of 60±0.1 volt

253 was applied across the specimens for 6 hours. The current was recorded every 30
254 minutes and the total charge was determined by integrating the current versus time plot.

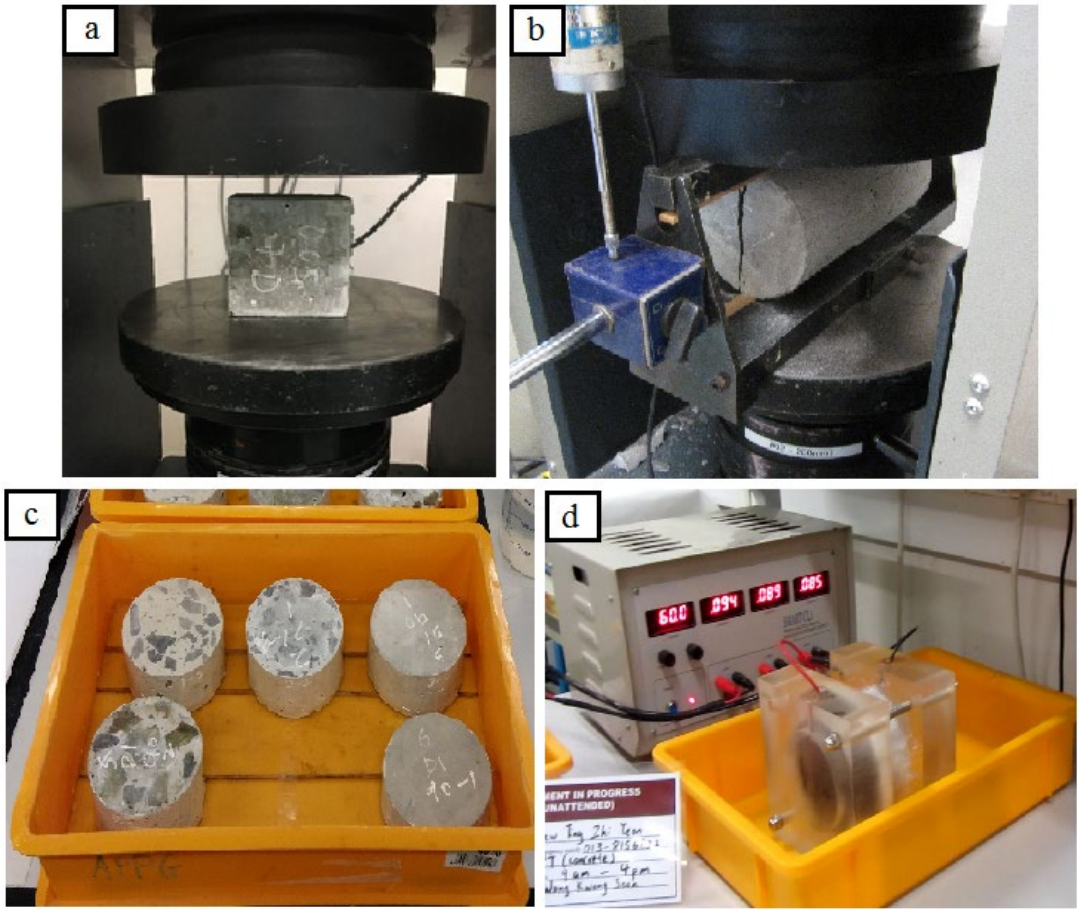

255

256 **Figure 4: Experimental setup for (a) compression, (b) splitting tensile, (c)**
257 **sorptivity and (d) rapid chloride penetration tests**

258

259 **3. Experimental results and discussion**

260 Table 5 presents test results for concrete mix no. 9–13 (center points in CCD). Based
261 on the results, the repeatability of experiment is examined. The discrepancy of all
262 concrete properties was small. The highest standard deviation was 6.21 mm for concrete
263 slump, 1.53 MPa for compressive strength, 0.11 MPa for splitting tensile strength,
264 0.13×10^{-3} mm/sec$^{1/2}$ for sorptivity and 16.7 C for chloride permeability. The coefficient

of variance ranged from 1.64% to 6.21%, indicating a small degree of dispersion over the mean. The analysis showed that the deviation of results was within the acceptable range and that the error of repeated tests was unlikely to result in imprecision.

Table 5: Repeatability of concrete properties in experiment

Concrete properties	Test results (FA20SF15)					Mean (n=5)	SD	COV (%)
	Mix no. 9	Mix no. 10	Mix no. 11	Mix no. 12	Mix no. 13			
Slump value (mm)	89	77	88	80	90	84.8	5.27	6.21
7-day compressive strength (MPa)	52.87	55.81	53.19	52.02	55.12	53.80	1.43	2.65
28-day compressive strength (MPa)	74.89	78.39	76.24	75.93	78.34	76.76	1.39	1.81
90-day compressive strength (MPa)	90.63	94.76	93.47	91.89	94.23	93.00	1.53	1.64
7-day splitting tensile strength (MPa)	3.44	3.69	3.71	3.59	3.62	3.61	0.09	2.63
28-day splitting tensile strength (MPa)	5.35	5.56	5.54	5.29	5.46	5.44	0.11	1.95
90-day splitting tensile strength (MPa)	6.03	6.28	6.23	6.01	6.17	6.14	0.11	1.77
28-day sorptivity ($mm/sec^{1/2}$ $x10^{-3}$)	3.12	2.96	2.91	2.99	2.71	2.94	0.13	4.55
90-day sorptivity ($mm/sec^{1/2}$ $x10^{-3}$)	2.90	2.80	2.71	2.82	2.60	2.77	0.10	3.64
180-day sorptivity ($mm/sec^{1/2}$ $x10^{-3}$)	2.54	2.49	2.42	2.49	2.42	2.47	0.05	1.92
28-day chloride permeability (C)	997.3	960.35	955.5	973.95	951.1	967.6	16.70	1.73
90-day chloride permeability (C)	702	681.9	670.5	701.6	660.1	683.2	16.66	2.44
180-day chloride permeability (C)	502	481.85	471.3	493	465	482.6	13.58	2.84

SD – Standard deviation; COV – Coefficient of variance

3.1. Workability of concrete

Figure 5 presents the workability of concrete assessed by the slump test. The slump value ranged from 30 mm to 247 mm, showing a significant impact of SF and FA on concrete workability. It decreased with an increase in the replacement level of SF in both binary and ternary blended concrete. Binary blended concrete containing 30% SF had the lowest slump value, which reduced the slump by 62% compared to the control mix. The reduction was caused by the large specific surface area of fine SF, which increased the water demand of concrete. The incorporation of SF also caused the concrete to become more cohesive and sticky, leading to a lower workability. The findings were in line with previous studies by Bagheri et al. [15] and Mazloom et al. [9]. Based on the result, it is not recommended to use an SF replacement level of more than 15% as this would cause the slump value to be below the minimum value of 50 mm suggested by the ACI standard for concrete pumping [35].

In contrast, the concrete slump value increased with the FA replacement level in both binary and ternary blended mixtures. For example, the binary blended concrete containing 40% FA achieved the highest slump value of 247 mm. This was due to the ball bearing effect provided by the round and smooth FA that reduced inter-particle friction in fresh concrete. Similar conclusion was also reached by Kwan and Chen [11], who observed a significant increase in the flow of cement paste that contained FA up to 40%.

For the combined effect, the workability of FA concrete decreased with an increase of SF content as shown in Figure 5 (c). The workability of FA40SF7.5, FA40SF15, FA40SF22.5 and FA40SF30 concrete was 41.8%, 59.6%, 63.6% and 71.2% respectively, below that of FA40 concrete. The use of SF increased the cohesiveness of

295 concrete resulting in a loss of workability [15]. Nevertheless, the disadvantage of SF
296 on workability could be overcome by increasing the content of FA as shown in Figure
297 5 (d). The slump value of FA10SF30, FA20SF30, FA30SF30 and FA40SF30 concrete
298 was 17.5 mm, 25.5 mm, 31.25 mm and 41.25 mm higher than that of SF30 concrete
299 respectively. The spherical FA particles acted as ball bearings between the concrete
300 mixtures to provide a lubricant effect [11].

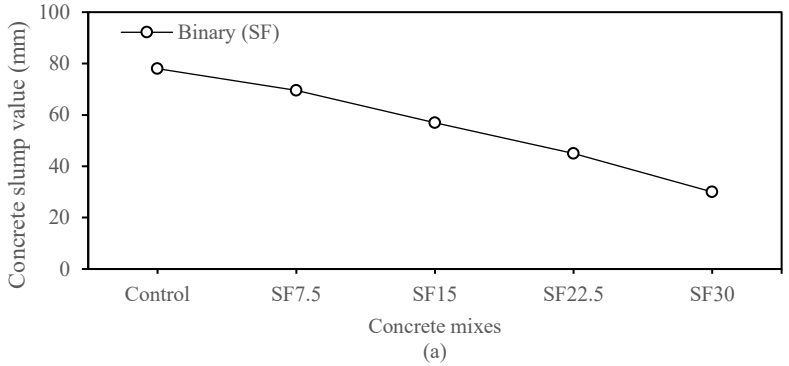

301

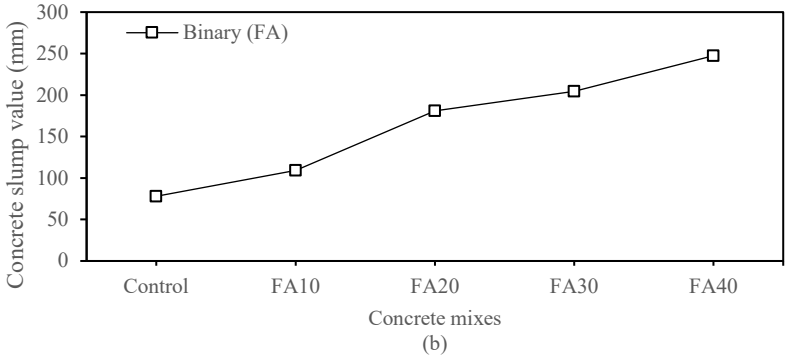

302

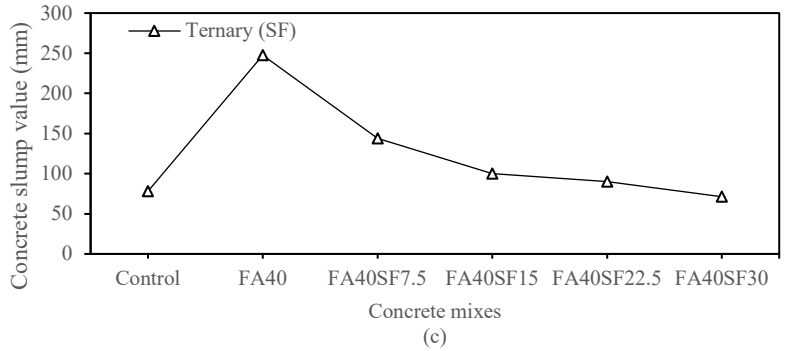

303

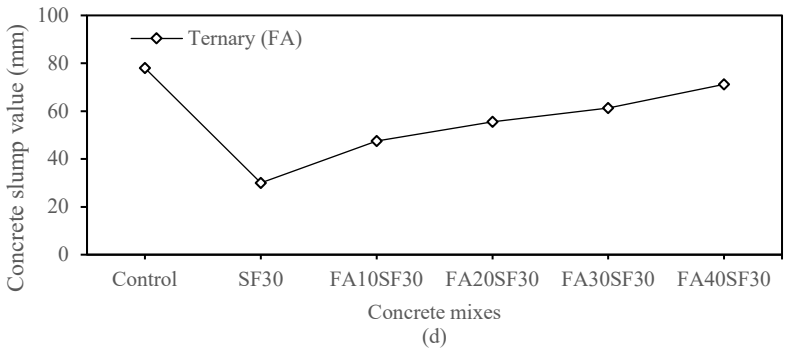

304

305 **Figure 5: Effects on workability of (a) SF in binary, (b) FA in binary, (c) SF in**
306 **ternary, and (d) FA in ternary blended concrete**

307

308 *3.2. Compressive strength of concrete*

309 The compressive strength of concrete determined after 7, 28 and 90 days of curing is
310 shown in Figure 6. The strength of all the concrete mixes increased orderly with the
311 curing time. Binary concrete blended with SF up to 15% of replacement level achieved
312 higher compressive strength than the control mix regardless of age. But the further
313 addition of SF led to a lower concrete strength than the control mix. The strength
314 increase at 7 days was 3.4% and 12.6% for SF7.5 and SF15 concrete respectively. This
315 was attributed to the pozzolanic reaction of fine SF, which reacted rapidly with calcium
316 hydroxide ($Ca(OH)_2$) from cement hydration to form calcium silicate hydrate (C-S-H).
317 However, the strength of the SF22.5 and SF30 concrete mixes decreased by 5.7% and
318 11.3% respectively. The result showed that the optimum SF content was between 15%
319 and 22.5%, above which there would be a shortage of $CaOH_2$ for pozzolanic reaction
320 [8]. The reduction of strength was also due to the increased concrete cohesiveness
321 resulting in a less homogeneous mixture. The results tied well with the studies of
322 Tripathi et al. [26] and Mazloom et al. [9] which showed an optimum dose of SF
323 between 15% and 25% in terms of compressive strength.

As for the effect of FA on binary blended concrete, the 7-day compressive strength decreased by 10.4%, 3.8%, 9.3% and 8.7% respectively for FA10, FA20, FA30 and FA40 mixes. However, the compressive strength improved with the curing time. At 90 days, these FA mixes had a higher strength than the control mix with a percentage of 0.7%, 2.4%, 4.7% and 1.5% respectively. FA had a particle size bigger than SF. As a result, the total surface area of FA particles was lower, which reduced the rate of pozzolanic reaction in order to gain strength. FA contained aluminium oxide and silicon dioxide in amorphous state, which reacted gradually with $Ca(OH)_2$ to form C-S-H. The result was consistent with the work of Sumer [13], Kondraivendhan and Bhattacharjee [36] and Alaka and Oyedele [37].

The results showed the synergistic effect of SF and FA on ternary blended concrete, which compensated for their individual limitations. SF improved compressive strength which offset the lower strength gain caused by FA at early age. The incorporation of 7.5% of SF as in FA40SF7.5 and 15% as in FA40SF15 improved the 7-day compressive strength of FA40 concrete by 2.0% and 3.3% respectively. In both cases, the SF incorporation also improved the 28-day strength by 3.3% and 4.3% as well as the 90-day strength by 1.0% and 3.0%. In addition to inducing pozzolanic reaction, the fine SF also acted as a filler to increase the nucleation of C-S-H which improved the strength gain [15]. The FA20SF15 concrete had the highest strength improvement of 8.4% at 28 days and 9.4% at 90 days compared to the control, though its 7-day compressive strength was 5.0% lower. This was due to the mutual interaction between the pozzolanic reaction of FA and the filler effect provided by SF. In addition, the effect of high-volume cement replacement was studied through the FA40SF15, FA20SF30, FA30SF30 and FA40SF30 mixes. The 90-day compressive strength of these concrete compared to the control mix was 4.5%, -1.7%, -15.04% and -21.8% respectively.

Although the compressive strength was reduced due to the use of high-volume FA and SF, the substitution was justified from a sustainability point of view.

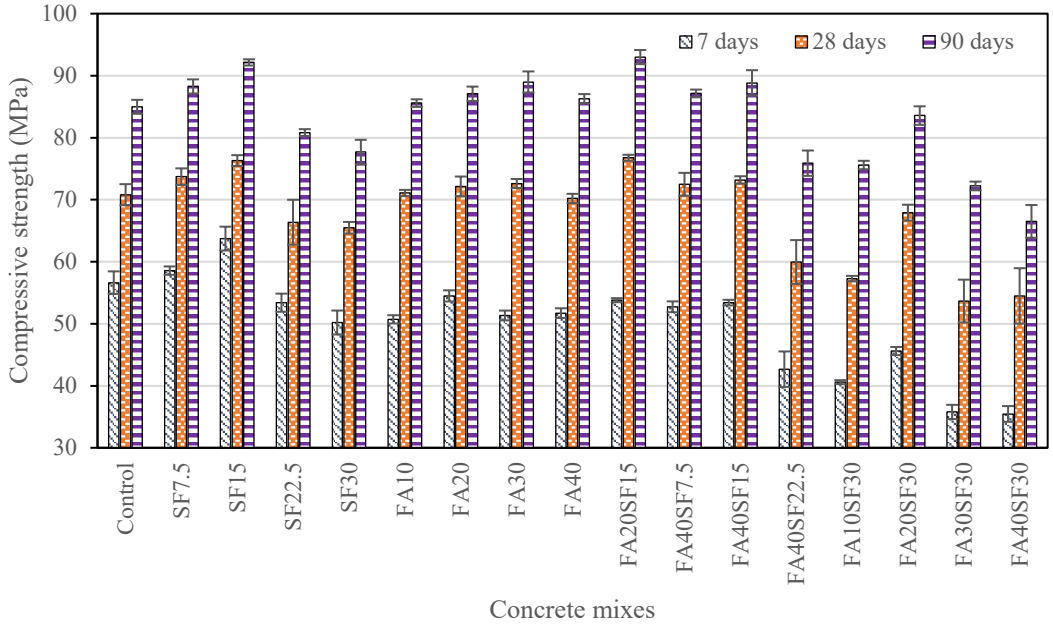

Figure 6: Effect of SF and FA on concrete compressive strength

3.3. Splitting tensile strength of concrete

Figure 7 shows the splitting tensile strength of binary and ternary blended concrete at 7, 28 and 90 days. The tensile strength increased with the curing time and it showed a similar result trend to that of the compressive strength. SF improved the tensile strength of binary blended concrete at both early and late ages, when the replacement level was 15% and below. The strength of SF15 concrete was 9.4%, 16.5% and 14.8% higher than the control mix at 7, 28 and 90 days respectively. This was in line with the work of Bhanja and Sengupta [8] who noticed an increase in splitting tensile strength if the SF replacement level was between 5% and 20%. The increase in early strength was

attributed to the fine SF, which provided a filler effect on the concrete pore. The strength gain was increased at a later age due to a more complete pozzolanic reaction of SF.

All replacement levels of FA lowered the 7-day tensile strength of binary blended concrete, but increased the strength at 28 and 90 days. The FA30 concrete achieved the highest 28-day and 90-day tensile strengths with an improvement of 8.7% and 6.0% respectively, though the 7-day strength was 9.6% lower than the control mix. The lower early strength was due to the slow pozzolanic reaction of FA, but the reaction gradually became more complete, resulting in more C-S-H formation and higher strength at the later age [38]. Thereafter, the result showed a declining trend of strength increase for the addition of FA above 30%. Further substitution of cement by FA resulted in a reduction of $Ca(OH)_2$ from hydration for use in pozzolanic reaction. Both the splitting tensile and compressive strengths indicated that the optimum dosage of FA in binary blended concrete was 30%.

The synergy of SF and FA in ternary blended concrete had a stronger effect on tensile strength. FA20SF15 concrete reached the highest strength improvement of 17.9% and 17.2% at 28 and 90 days, respectively, and had a comparable 7-day strength of control concrete. The filler effect of SF compensated for the lower early strength caused by FA and the pozzolanic reaction of FA further increased the strength at the later age [15]. The incorporation of FA improved the tensile strength of SF concrete at a later age, as seen in the FA10SF30, FA20SF30 and FA30SF30 mixes by 0.6%, 3.8% and 0.9% respectively, relative to the SF30 mix. The results also showed an increase in the tensile strength of FA concrete due to the addition of SF. For example, the 7-day tensile strength of FA40SF7.5 and FA40SF15 concrete was 10.4% and 9.3%, respectively,

388 higher than FA40 concrete. However, a further substitution of SF and FA above 60%
389 in ternary blended concrete resulted in a severe reduction of strength. Dave et al. [39]
390 found that the substitution of quaternary binder above 50% was not effective in
391 improving concrete tensile strength. This was due to the lack of $Ca(OH)_2$ content for
392 pozzolanic reaction to provide bonding strength.

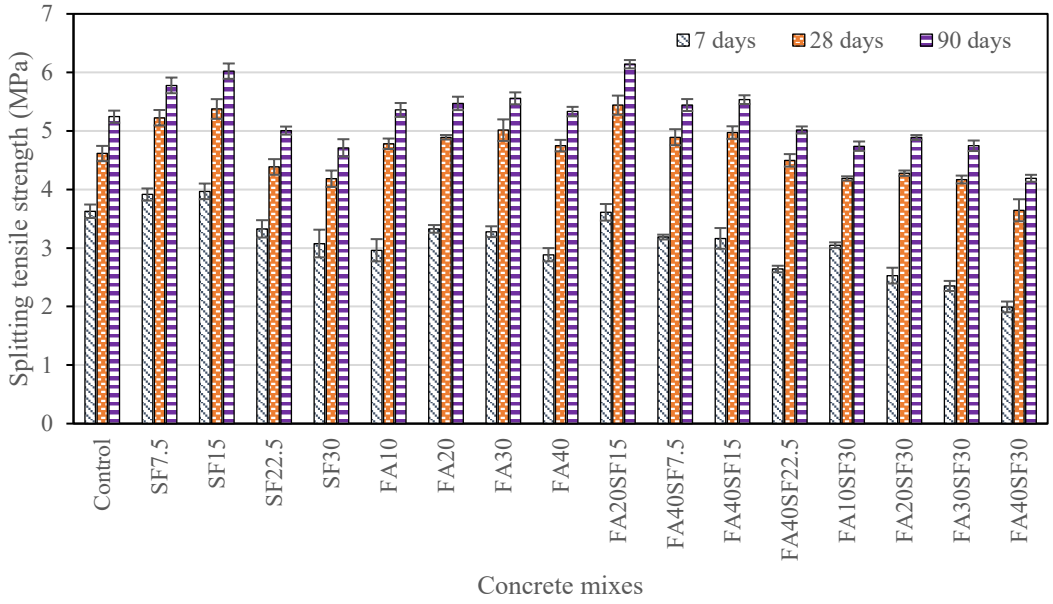

393

394 **Figure 7: Effect of SF and FA on splitting tensile strength of concrete**

395

396 *3.4. Sorptivity of concrete*

397 The rate of water absorption of concrete was studied using the sorptivity test. Figure 8
398 presents the sorptivity of concrete determined after 28, 90 and 180 days of curing. The
399 sorptivity of all concrete mixes decreased with the curing time, indicating an improved
400 durability over time. More complete hydration of concrete was achieved at a later age
401 which densified concrete pore due to the formation of C-S-H.

The incorporation of SF with a percentage of up to 15% improved the sorptivity of binary blended concrete. The extent of improvement in sorptivity decreased with an increase in the SF replacement level. The SF22.5 concrete had a similar sorptivity to the control concrete. Further incorporation of SF up to 30% increased sorptivity by 15.6%, 36.6% and 47.1% at 28, 90 and 180 days respectively, indicating reduced durability. The decrease in sorptivity at a lower SF content was due to the filling of concrete pore by fine SF, which improved the microstructural fineness. Bagheri et al. [15] demonstrated that the SF reduced the pore connectivity of concrete. The pore structure of concrete was also enhanced by the pozzolanic reaction of SF. Meanwhile, higher sorptivity at a higher SF content was due to more pores caused by the high cohesiveness of concrete.

The sorptivity of all binary concrete blended with FA was below that of control concrete at all ages. For example, the improvement in sorptivity was 4.1%, 19.9%, 16.7% and 8.4% for FA10, FA20, FA30 and FA40 concrete respectively at 180 days. This was due to the pozzolanic reaction of FA, which densified the concrete pore with more C-S-H formation. Ponikiewski and Gołaszewski [12] also demonstrated that the addition of FA reduced the water absorption of concrete by creating a more compact pore structure through the pozzolanic reaction. The results confirmed that the compressive and tensile strength of FA concrete improved with age.

As for ternary blended concrete, the results mostly showed higher sorptivity than control concrete, with the exception of FA20SF15, FA40SF7.5 and FA40SF7.5 mixes. This was due to the high level of OPC replacement by SF and FA, where the resulting concrete was deficient in $Ca(OH)_2$ for pozzolanic reaction. Nonetheless, FA20SF15 and FA40SF7.5 concrete improved the 180-day sorptivity by 20.3% and 6.8% respectively,

while FA40SF15 concrete had comparable sorptivity to the control mix. The findings tied well with the study by Radlinski and Olek [14] which showed a substantial improvement in sorptivity when 20% FA and 15% SF were incorporated. Besides, the incorporation of FA also improved the sorptivity of SF concrete. For example, FA10SF30, FA20SF30 and FA30SF30 concrete reduced the 90-day sorptivity of SF30 concrete by 5.2%, 5.4% and 2.5% respectively. The pozzolanic reaction of FA filled up the concrete pore. In terms of durability, it is not recommended to substitute OPC with SF and FA in high volume.

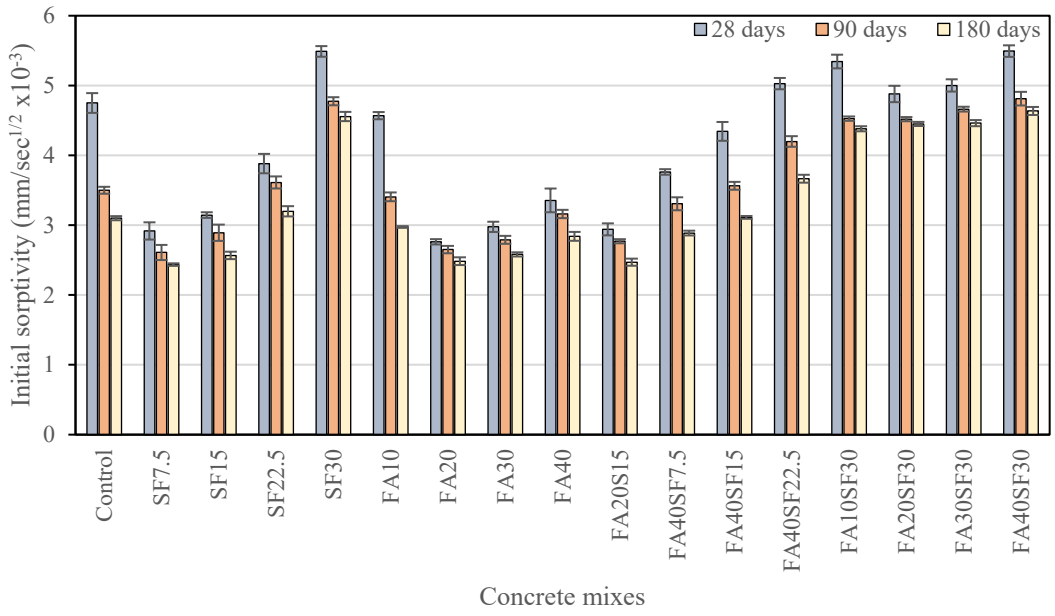

Figure 8: Effect of SF and FA on concrete sorptivity

3.5. Chloride permeability of concrete

The chloride permeability expressed as the charge passed through concrete is determined by the rapid chloride penetration test (RCPT). Figure 9 presents the chloride

permeability of binary and ternary concrete blended with SF and FA at 28, 90 and 180 days. The chloride permeability of concrete decreased over time due to more complete hydration.

The result showed that the chloride permeability of binary concrete blended with SF decreased with an increase in the replacement level. SF30 concrete had the largest reduction in chloride permeability, which was 67.3%, 59.9% and 59.0% lower than control concrete at 28, 90 and 180 days respectively. As for FA in binary blended concrete, chloride permeability also decreased with an increase in FA content. FA concrete showed a slightly lower reduction than SF concrete. FA40 concrete had the largest reduction in chloride permeability, which was 59.9%, 51.1% and 49.0% lower than control concrete at 28, 90 and 180 days respectively.

The result showed that ternary blended concrete had a combined effect of SF and FA on minimizing chloride permeability. Chloride permeability decreased with the total replacement level of SF and FA. In this regard, FA40SF30 concrete achieved the lowest chloride permeability with a reduction of 70.1%, 63.9% and 62.5% at 28, 90 and 180 days respectively compared to control concrete. Dave et al. [39] and Radlinski and Olek [14] found that the reduction in chloride permeability was due to the pozzolanic reactions of SF and FA, which reduced capillary pores and compacted the concrete pore structure. This result was slightly different from the findings of sorptivity test described in Section 3.4. This was attributed to the modification of chemical composition in concrete as a result of the incorporation of SF and FA. SF and FA diluted concrete pore solution and reduced hydroxide (OH^-) concentration of concrete. In this case, RCPT, which measured electric current based on hydroxide (OH^-) and chloride (Cl^-) ions, was influenced by pore solution chemistry. Neithalath and Jain [40] found that when

supplementary cementitious material such as SF was used in RCPT, 70% of permeability improvement was attributed to pore refinement, while another 30% was due to a reduction in concrete alkalinity. Nevertheless, the result still showed that the chloride permeability of FA20SF15 concrete decreased by 60.9%, 53.5% and 50.1% at 28, 90 and 180 days respectively compared to the control. It is necessary to perform other test, such as the sorptivity test, to complement the RCPT in assessing concrete durability.

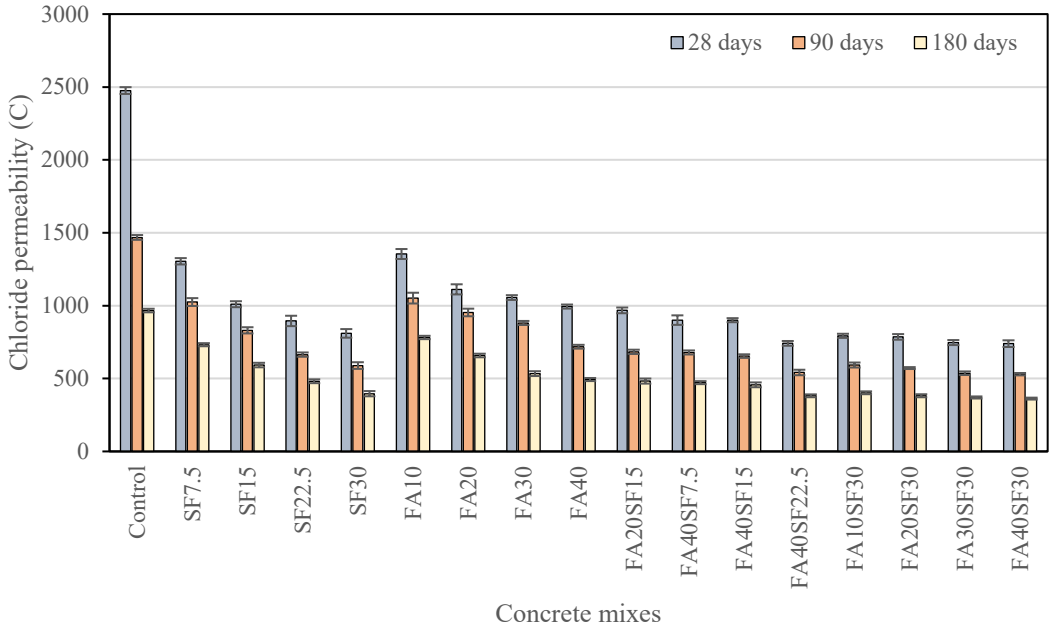

Figure 9: Effect SF and FA on chloride permeability of concrete

3.6. Comparison with limestone concrete

Figure 10 shows the development of compressive strength of the limestone and control concrete. Both types of concrete increased in strength with the curing time, but the

strength gain slowly decreased. Concrete compressive strength at 1, 7 and 28 days was approximately 40%, 70% and 80% of 90-day strength respectively. This showed that the hydration became more complete as the concrete aged. The strength of limestone concrete was slightly higher than that of control concrete. The percentage difference was 11.7%, 10.6%, 8.5%, 4.1%, 4.7% and 5.2% at 1, 7, 14, 28, 56 and 90 days respectively. This was ascribed to stronger aggregate characteristics of limestone than SiMn slag. The limestone aggregate had a higher abrasion resistance than SiMn slag as shown in Table 2, which produced a higher strength concrete. The findings were consistent with the study of Kılıç et al. [41], in which the concrete compressive strength improved when a stronger aggregate was used.

The strength difference between the two concrete types was constant at various ages. The average strength difference was 4.33 MPa and the standard deviation was 1.03 MPa, indicating a fairly linear strength relationship between limestone and control concrete. In this context, the correlation between the compressive strength of the two concrete types was established by means of a regression analysis as shown in Figure 11. The two compressive strengths were presented as a linear equation in Eq. (2).

$$f_{c,LS} = 0.991 f_{c,SM} + 4.9027 \quad (2)$$

In Eq. (2), $f_{c,LS}$ represents the compressive strength of limestone concrete and $f_{c,SM}$ refers to the compressive strength of control concrete. The established correlation has an R^2 value of 0.9963, indicating a high fitness for the regression model. The equation can be used to estimate the compressive strength of limestone concrete based on that of SiMn slag concrete and vice versa.

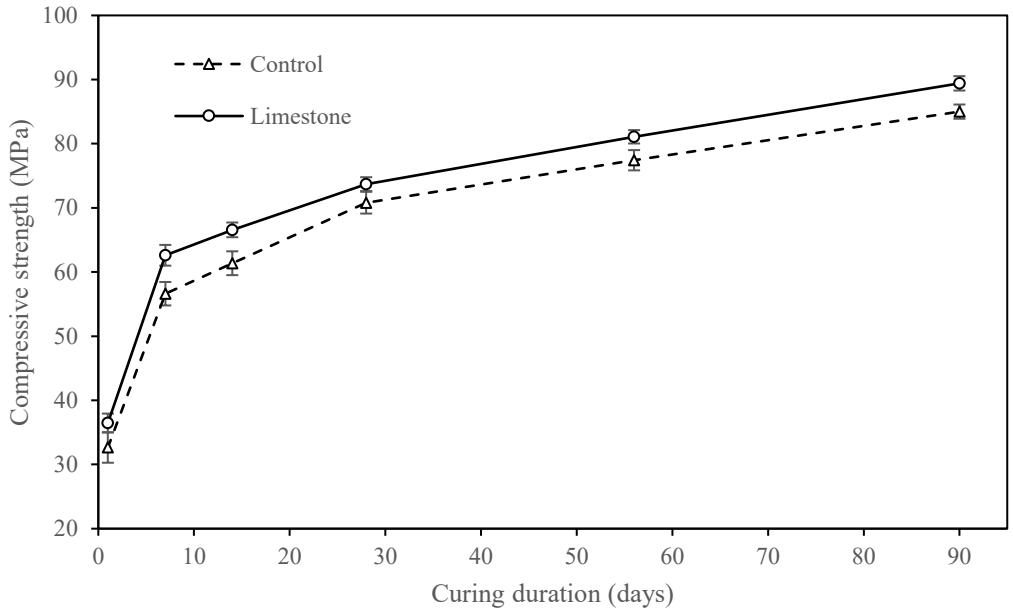

501

502 **Figure 10: Limestone and control concrete compressive strength**

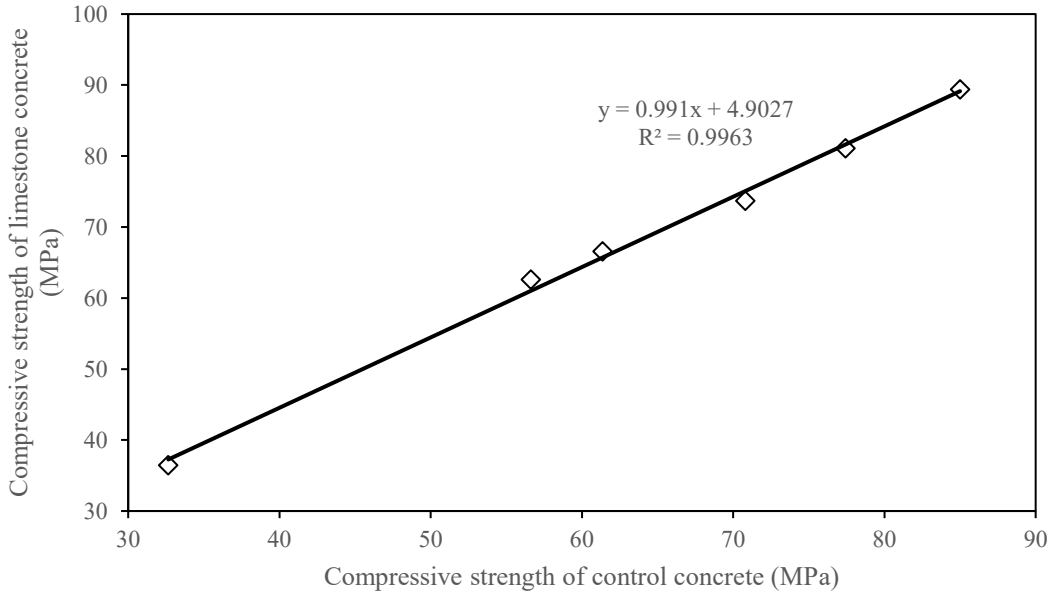

503

504 **Figure 11: Correlation of compressive strength between limestone and control**
505 **concrete**

506

4. Development of prediction model using RSM

4.1. Mathematical prediction model for concrete properties

Concrete properties in terms of compressive strength, splitting tensile strength, sorptivity, chloride permeability and workability of concrete presented previously were inputs to the development of prediction model. The RSM was used to perform statistical analysis and to establish the relationship between these concrete properties and the SF and FA contents. The resulting prediction models are summarized in Table 6. These models were expressed as polynomial functions of x_1 as FA/B and x_2 as SF/B, which were the ratio of FA and SF content to total binder content.

Prediction models for compressive strength and splitting tensile strength at 7, 28 and 90 days were all expressed as quadratic polynomial functions of FA/B and SF/B. The models showed that SF/B contributed significantly to the strength of both early and later ages. In contrast, FA/B had a less significant effect on 7-day strength, but its effect was more prominent on 28-day and 90-day strengths. As such, the polynomial coefficients of FA/B increased with concrete age, indicating that the parameter had a higher influence. The result was in line with the statistical models of Aldahdooh et al. [25], Nehdi and Summer [18] and Bayramov et al. [42], which showed that quadratic functions were suitable for describing the relationship between concrete strength and supplementary cementitious materials content.

Sorptivity at 28, 90 and 180 days was formulated as cubic equations. The models showed a decrease in sorptivity as FA/B and SF/B increased until the optimum point was reached. SF/B had a steeper curve slope than FA/B, indicating its greater effect on the sorptivity. The degree of polynomial equations for sorptivity was higher than that of Güneyisi et al. [20] and Rezaifar et al. [21], who developed linear and quadratic

531 models respectively in their studies. This was due to a wider range of variables being
532 investigated in this study.

533 As for chloride permeability, the 28-day and 90-day prediction models were quartic
534 equations, and the 180-day model was cubic. The use of quartic models was due to the
535 sudden reduction of chloride permeability of concrete with only slight incorporation of
536 SF and FA at 28 and 90 days. This confirmed that the decrease in chloride permeability
537 was caused by modification of pore chemistry rather than pore refining contributed by
538 SF and FA. Nonetheless, the 180-day chloride permeability equation was more similar
539 to the sorptivity equation since the pore refining effect caused by pozzolanic reaction
540 of SF and FA was more pronounced.

541 Concrete slump value was formulated as a cubic equation, showing a non-linear
542 relationship to SF and FA. The equation indicated that the increased use of SF greatly
543 decreased the slump value, but the use of FA improved the slump value. Sonebi [43]
544 showed that fresh properties of concrete could be expressed as cubic functions of FA
545 content, OPC content, superplasticizer dosage and w/b ratio. Lotfy et al. [44] used
546 quadratic equations for the relationship between fresh properties and concrete variables.

547

548 **Table 6: Prediction model for concrete properties**

Parameter	Compressive strength (MPa)			Splitting tensile strength (MPa)			
	7-day	28-day	90-day	7-day	28-day	90-day	
Polynomial degree	Quadratic	Quadratic	Quadratic	Quadratic	Quadratic	Quadratic	
Constant	55.63	69.20	82.78	3.43	4.62	5.19	
x_1	-24.19	39.56	60.37	-0.29	3.79	4.39	
x_2	79.55	97.42	107.07	7.32	8.77	9.67	
x_1x_2	-83.34	-86.39	-98.58	-4.69	-3.19	-2.94	
x_1^2	36.51	-93.09	-135.85	-2.34	-9.32	-11.18	
x_2^2	-340.67	-404.45	-425.90	-28.65	-35.57	-38.91	
Parameter	Sorptivity (mm/sec$^{1/2}$ x10^{-3})			Chloride permeability (C x10^3)			Slump value (mm)
	28-day	90-day	180-day	28-day	90-day	180-day	
Polynomial degree	Cubic	Cubic	Cubic	Quartic	Quartic	Cubic	Cubic
Constant	4.82	3.56	3.14	2.47	1.47	0.96	77.51
x_1	-3.97	-4.13	-3.36	-17.99	-6.74	-1.77	455.76
x_2	-34.49	-18.12	-12.70	-26.39	-9.50	-3.12	-381.08
x_1x_2	92.55	43.01	32.60	138.86	35.04	10.06	-3147.72
x_1^2	-41.102	-3.61	-1.02	85.34	32.67	0.69	27.87
x_2^2	172.81	101.11	54.58	185.39	65.29	4.61	2589.18
$x_1x_2^2$	-227.56	-102.70	-75.11	-418.03	-81.54	-12.15	6857.14
$x_1^2x_2$	-30.50	-20.81	-17.05	-312.37	-92.01	-7.31	172.62
x_1^3	105.87	29.06	19.20	-174.47	-68.48	2.08	-311.91
x_2^3	-168.69	-91.35	11.24	-606.22	-258.27	-1.36	-6195.41
$x_1x_2^3$				450.27	120.54		
$x_1^2x_2^2$				353.79	5.08		
$x_1^3x_2$				251.72	128.28		
x_2^4				733.30	379.13		

x_1 denotes independent variable FA/B.

x_2 denotes independent variable SF/B.

549

550 *4.2. Evaluation of model fitness based on ANOVA*

551 The fitness of mathematical prediction models was evaluated using the two-way
552 analysis of variance (ANOVA). The ANOVA determined the significance of model and
553 variables on the responses through the F-test. The p-value at the significance level of
554 0.05 was used to determine the validity of null hypothesis. The null hypotheses were
555 established if the variable had no effect on the response and if the interaction between
556 variables had no effect on the response. When the p-value from F-test was not zero and
557 less than 0.05, the null hypothesis was rejected and the variables were regarded as
558 statistically significant.

559 Table 7, Table 8 and Table 9 summarize the outcomes of ANOVA for concrete strength,
560 durability and workability prediction models respectively. The result showed that the
561 variable SF/B for all models had a p-value of less than 0.05 and was statistically
562 significant. Thus, SF/B was included in the prediction models. On the contrary, FA/B
563 was tested as an insignificant variable with the exception of 7-day strengths, 28-day
564 chloride permeability and 180-day chloride permeability models. Exclusion of
565 insignificant variables might improve the prediction model. However, in this study, it
566 reduced the overall accuracy of model prediction and as such the variables were not
567 excluded. Lotfy et al. [44] had used all the variables, including those not significant, in
568 the models to enhance their accuracy. Higher degree polynomial variables and
569 interactions between them were similarly assessed, but results were not shown to avoid
570 lengthy paper contents. Furthermore, the ANOVA showed that the lack of fit of all
571 models had p-value of more than 0.05, indicating that it was not significant. The lack
572 of model fitness did not cause residual errors. The mean square of pure error was less
573 than that of model and also, in general, that of lack of fit, which showed that the error
574 between the replicate runs was minimal.

575 Table 10 shows the fit statistics for prediction models. The coefficient of determination
576 (R^2) of all models ranged from 0.853 to 0.999. These R^2 values were close to 1,
577 indicating that the regression models fit the data points. The 7-day, 28-day and 90-day
578 compressive strength models had marginally lower R^2 values of 0.896, 0.853 and 0.895
579 respectively. This was ascribed to a higher sensitivity of high strength concrete to the
580 material variations and testing environment. The adjusted R^2 and predicted R^2 were
581 used to justify the inclusion of insignificant variables in the model. When insignificant
582 variables were included, the adjusted R^2 plateaued. The predicted R^2 decreased if too
583 many insignificant terms were included. The difference between adjusted and predicted
584 R^2 should be less than 0.2 in order to limit the number of insignificant terms and to
585 ensure the reliability of prediction [24]. The 28-day compressive strength model had
586 the largest difference between two R^2s of 0.106. The difference for all models was
587 below this value, indicating that the addition of insignificant terms had no negative
588 influence on the prediction. Besides, the adequate precision of all models was well
589 above 4, showing that the models had a low prediction error and were therefore
590 sufficiently fit for optimization [45].

591 In summary, the ANOVA showed that null hypotheses were rejected for all models and
592 that the models were statistically significant. The models contained all important terms
593 required by ANOVA and were therefore adequate to describe the relationship between
594 variables and responses.

595

596 **Table 7: ANOVA of prediction model for concrete strength**

Response	Source	Sum of square	Mean square	F-value	p-value	Significance
7-day compressive strength	Model	902.76	180.55	25.86	0.0001	Yes
	FA/B	214.70	214.70	30.75	0.0001	Yes
	SF/B	382.63	382.63	54.81	0.0001	Yes
	Lack of fit	94.53	8.59	3.37	0.1257	No
	Pure error	10.19	2.55	-	-	-
28-day compressive strength	Model	959.97	191.99	17.38	0.0001	Yes
	FA/B	49.78	49.78	4.51	0.0508	No
	SF/B	419.87	419.87	38.01	0.0001	Yes
	Lack of fit	156.10	14.19	5.91	0.0504	No
	Pure error	9.61	2.40	-	-	-
90-day compressive strength	Model	1060.03	212.01	25.58	0.0001	Yes
	FA/B	33.78	33.78	4.08	0.0618	No
	SF/B	404.32	404.32	48.78	0.0001	Yes
	Lack of fit	112.64	10.24	3.51	0.1185	No
	Pure error	11.68	2.92	-	-	-
7-day splitting tensile strength	Model	4.90	0.98	32.85	0.0001	Yes
	FA/B	1.63	1.63	54.78	0.0001	Yes
	SF/B	1.21	1.21	40.70	0.0001	Yes
	Lack of fit	0.40	0.04	3.19	0.1369	No
	Pure error	0.05	0.01	-	-	-
28-day splitting tensile strength	Model	5.38	1.08	39.50	0.0001	Yes
	FA/B	0.08	0.08	2.86	0.1117	No
	SF/B	1.60	1.60	58.89	0.0001	Yes
	Lack of fit	0.35	0.03	2.32	0.2168	No
	Pure error	0.06	0.01	-	-	-
90-day splitting tensile strength	Model	6.35	1.27	44.18	0.0001	Yes
	FA/B	0.12	0.12	4.14	0.0598	No
	SF/B	1.66	1.66	57.78	0.0001	Yes
	Lack of fit	0.37	0.03	2.36	0.2111	No
	Pure error	0.06	0.01	-	-	-

597

598

599 **Table 8: ANOVA of prediction model for concrete durability**

Response	Source	Sum of square	Mean square	F-value	p-value	Significance
28-day sorptivity	Model	199.38 $x10^{-7}$	22.15 $x10^{-7}$	34.15	0.0001	Yes
	FA/B	0.01 $x10^{-7}$	0.01 $x10^{-7}$	0.14	0.7109	No
	SF/B	8.08 $x10^{-7}$	8.08 $x10^{-7}$	12.46	0.0047	Yes
	Lack of fit	6.24 $x10^{-7}$	0.89 $x10^{-7}$	4.00	0.0993	No
	Pure error	0.89 $x10^{-7}$	0.22 $x10^{-7}$	-	-	-
90-day sorptivity	Model	23.20 $x10^{-7}$	13.69 $x10^{-7}$	63.42	0.0001	Yes
	FA/B	0.10 $x10^{-7}$	0.10 $x10^{-7}$	0.49	0.5003	No
	SF/B	5.15 $x10^{-7}$	5.15 $x10^{-7}$	23.85	0.0005	Yes
	Lack of fit	1.87 $x10^{-7}$	0.27 $x10^{-7}$	2.11	0.2450	No
	Pure error	0.51 $x10^{-7}$	0.13 $x10^{-7}$	-	-	-
180-day sorptivity	Model	134.21 $x10^{-7}$	14.91 $x10^{-7}$	208.91	0.0001	Yes
	FA/B	0.01 $x10^{-7}$	0.01 $x10^{-7}$	1.13	0.3115	No
	SF/B	2.91 $x10^{-7}$	2.91 $x10^{-7}$	40.73	0.0001	Yes
	Lack of fit	0.67 $x10^{-7}$	0.01 $x10^{-7}$	3.40	0.1271	No
	Pure error	0.11 $x10^{-7}$	0.03 $x10^{-7}$	-	-	-
28-day chloride permeability	Model	2.76 $x10^{6}$	1.97 $x10^{5}$	468.51	0.0001	Yes
	FA/B	20955.03	20955.03	49.80	0.0004	Yes
	SF/B	4808.75	4808.75	11.43	0.0148	Yes
	Lack of fit	1130.85	565.42	1.62	0.3048	No
	Pure error	1393.63	348.41	-	-	-
90-day chloride permeability	Model	1.01 $x10^{6}$	72242.33	283.09	0.0001	Yes
	FA/B	351.70	351.70	1.38	0.2849	No
	SF/B	10236.72	10236.72	40.11	0.0007	Yes
	Lack of fit	142.55	71.27	0.21	0.8225	No
	Pure error	1388.59	347.15	-	-	-
180-day chloride permeability	Model	4.66 $x10^{5}$	51760.64	226.18	0.0001	Yes
	FA/B	3125.99	3125.99	13.66	0.0035	Yes
	SF/B	6135.65	6135.65	26.81	0.0003	Yes
	Lack of fit	1594.74	227.82	0.99	0.5380	No
	Pure error	922.53	230.63	-	-	-

600

601

602 **Table 9: ANOVA of prediction model for concrete workability**

Response	Source	Sum of square	Mean square	F-value	p-value	Significance
Slump value	Model	59691.43	6632.38	84.26	0.0001	Yes
	FA/B	231.80	231.80	2.94	0.1142	No
	SF/B	478.86	478.86	6.08	0.0313	Yes
	Lack of fit	727.09	103.87	2.99	0.1531	No
	Pure error	138.80	34.70	-	-	-

603

604 **Table 10: Fit statistics of prediction model**

Response	R^2	Adjusted R^2	Predicted R^2	Adequate precision	Estimated error (95% CI)
7-day compressive strength	0.896	0.861	0.806	17.63	±2.28 MPa
28-day compressive strength	0.853	0.804	0.698	13.35	±2.87 MPa
90-day compressive strength	0.895	0.860	0.797	16.76	±2.48 MPa
7-day splitting tensile strength	0.916	0.888	0.830	20.46	±0.15 MPa
28-day splitting tensile strength	0.929	0.906	0.862	19.67	±0.14 MPa
90-day splitting tensile strength	0.936	0.915	0.872	21.01	±0.15 MPa
28-day sorptivity	0.965	0.937	0.861	15.61	$\pm 0.23 \times 10^{-3}$ mm/sec$^{0.5}$
90-day sorptivity	0.981	0.966	0.917	21.01	$\pm 0.13 \times 10^{-3}$ mm/sec$^{0.5}$
180-day sorptivity	0.994	0.989	0.973	37.35	$\pm 0.08 \times 10^{-3}$ mm/sec$^{0.5}$
28-day chloride permeability	0.999	0.997	0.924	100.21	±22.45 C
90-day chloride permeability	0.999	0.995	0.972	69.34	±17.48 C
180-day chloride permeability	0.995	0.990	0.975	57.78	±13.47 C
Slump value	0.986	0.974	0.940	35.18	±7.90 mm

605

606

5. Optimization, validation and application of prediction model

5.1. Optimization of concrete properties with experimental validation

The optimization of concrete properties was carried out using the prediction models in Table 6 developed from RSM. Table 11 presents the criteria of optimization for variables and responses. The main objective of optimization was to maximize compressive and splitting tensile strengths, and to minimize soprtivity and chloride permeability of concrete. The optimization was carried out over the feasible ranges of SF/B and FA/B as 0 to 0.3 and 0 to 0.4 respectively. The slump value was targeted to fall between 80 mm and 210 mm, with the lower limit being set for concrete pumping and the upper limit being recommended by BS EN 12350-2 [46].

In the optimization process, SF/B and FA/B were varied simultaneously in order to compute the combination of variables that achieved the optimization objective. The optimization process also considered the interaction of the responses. These responses were expressed as a composite desirability function determined from the geometric mean desirability of individual responses [47]. The desirability function could range from 0 to 1, with 0 indicated an outside-of-range prediction and 1 denoted an ideal prediction. The optimization was therefore performed by maximizing the desirability.

Optimum values of SF/B as 0.115 and FA/B as 0.163 were obtained from the optimization process. Figure 12 shows a graphical illustration of the desirability function. The desirability of optimization was 0.896. The region bounded by FA/B of 0.1–0.3 and SF/B of 0.06–0.18 generally had a high desirability of more than 0.8. FA/B had a more significant effect to achieve a higher optimization desirability. It was found that when SF/B was zero, the use of FA/B between 0.1 and 0.4 could still result in a

desirability between 0.61 and 0.75. In contrast, the desirability function illustrated that when FA/B was zero, the use of SF/B at all levels resulted in zero desirability.

Experiments were again conducted to validate the optimization outcomes. All concrete properties predicted by the models were tested in the validation experiment. Materials from the same source were used. Concrete mix proportions were amended by using SF/B as 0.115 and FA/B as 0.163. In all experiments, the same procedures and conditions described in Section 2.4 were used.

Figure 13 shows the results of validation tests using the optimum SF and FA contents, as well as the comparison with the predicted results and limestone concrete determined by Ting et al. [7]. In terms of strength, concrete generally achieved a higher experimental value than the predicted outcome. The 7-day compressive strength had the highest error of 3.4%. The experimental sorptivity was close to the predicted value. The 90-day sorptivity had the highest error of 4.9%. As for chloride permeability, the 28-day results showed a higher error of 18.0%. This was attributed to the limited design points to consider the sensitivity of the model to OH^- and Cl^- ions related chemistry in concrete caused by SF and FA. The drawback of CCD method was that the effect of variables within the box of CCD (Figure 2) on response was not covered by the model development. The optimum SF and FA contents that fell within this region caused less accurate prediction of chloride permeability. Nonetheless, the error decreased at an older age to 9.1% and 10.3% respectively for 90-day and 180-day chloride permeability.

The validation study proves that the optimum SF and FA contents of 11.5% and 16.3% respectively are compatible with the optimization outcome. The optimization of SF and FA improves the hardened state properties of SiMn slag concrete. In this regard, the 90-

day compressive strength, 90-day tensile strength, 180-day sorptivity and 180-day chloride permeability are improved by 10.4%, 18.9%, 24.9% and 44.6% respectively.

According to Ting et al. [7], SiMn slag concrete without the inclusion of SF and FA had a lower strength and early-age durability than limestone concrete. For example, its 90-day compressive strength and 28-day chloride permeability were 7.0% and 9.8% lower than that of limestone concrete. In this study, however, the use of SF and FA at the optimum replacement level overcomes the limitations of SiMn slag concrete. The 90-day compressive strength, 90-day tensile strength, 180-day sorptivity and 180-day chloride permeability have been improved by 4.2%, 1.6%, 27.3% and 24.0% respectively, compared to limestone concrete.

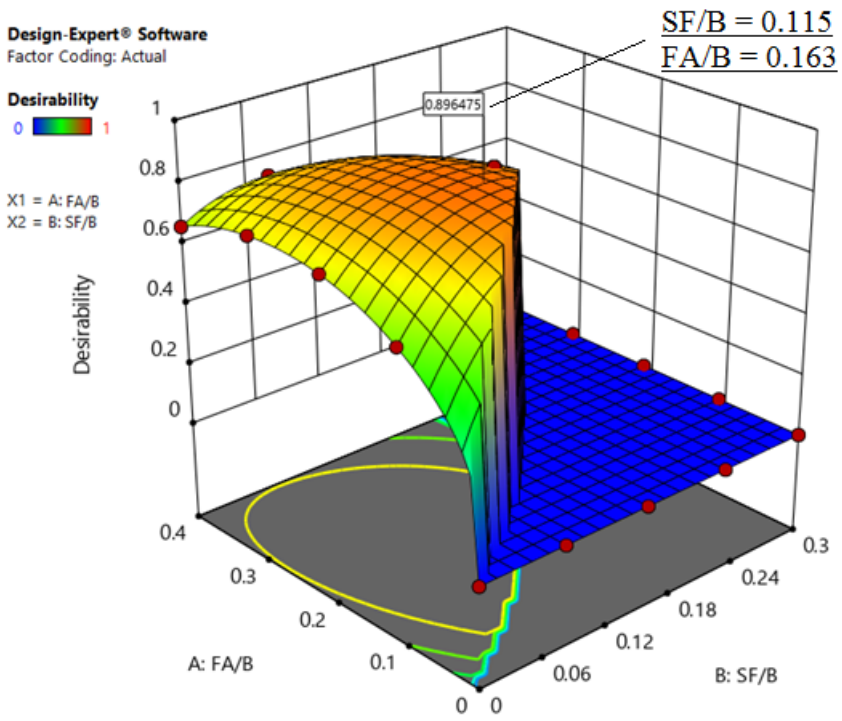

Figure 12: Desirability function of optimization

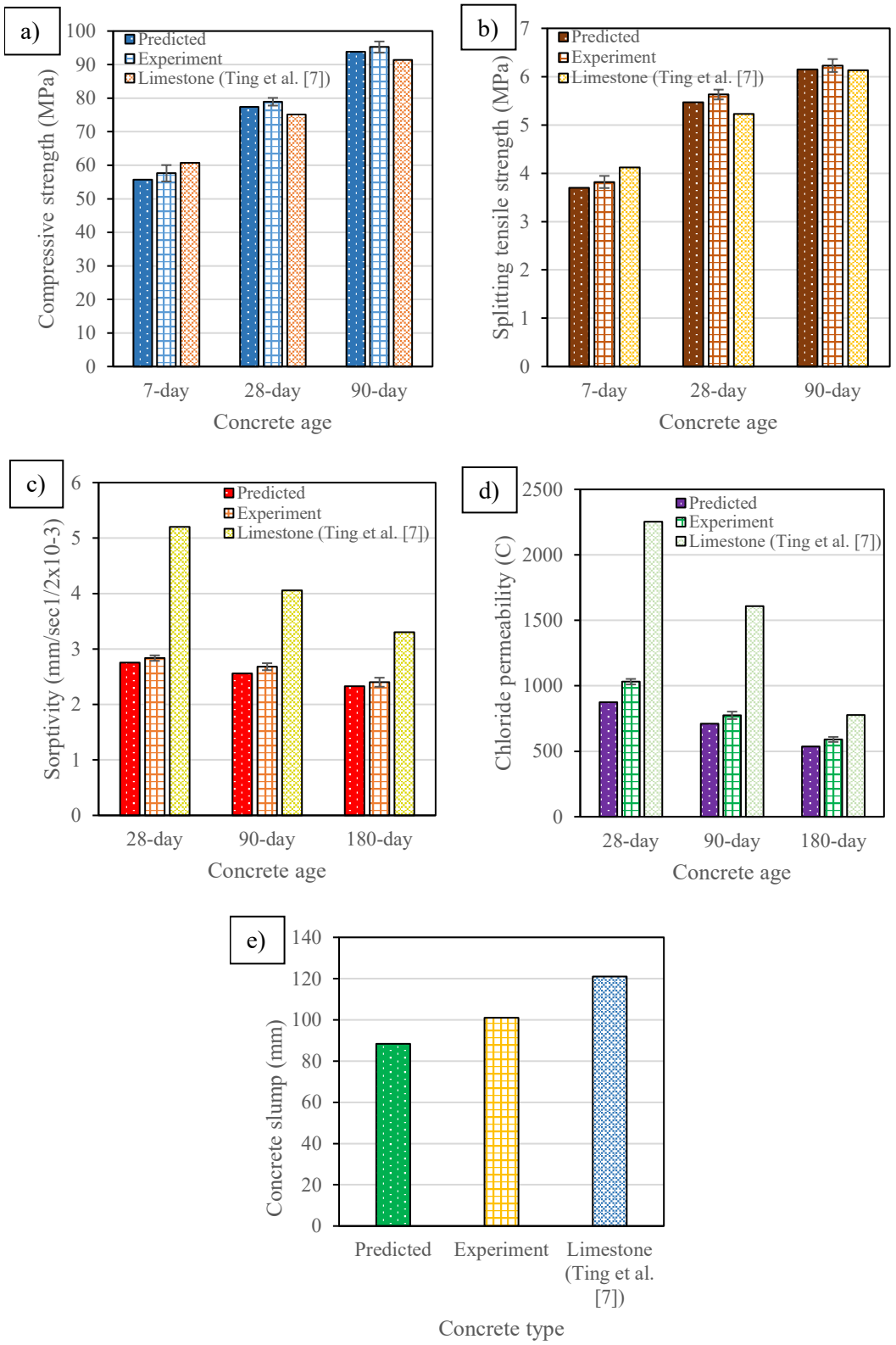

Figure 13: Predicted and experiment results and comparison with limestone concrete in terms of a) compressive strength, b) tensile strength, c) sorptivity, d) chloride permeability and e) concrete slump

671 **Table 11: Optimization criteria for variables and responses**

Variable and response	Optimization target	Lower limit	Upper limit
FA/B	Within range	0	0.4
SF/B	Within range	0	0.3
7-day compressive strength (MPa)	Maximize	35.46	63.73
28-day compressive strength (MPa)	Maximize	53.66	78.39
90-day compressive strength (MPa)	Maximize	66.50	94.76
7-day splitting tensile strength (MPa)	Maximize	1.99	3.97
28-day splitting tensile strength (MPa)	Maximize	3.64	5.56
90-day splitting tensile strength (MPa)	Maximize	4.19	6.28
28-day sorptivity ($mm/sec^{0.5}$ $x10^{-3}$)	Minimize	2.713	5.493
90-day sorptivity ($mm/sec^{0.5}$ $x10^{-3}$)	Minimize	2.604	4.812
180-day sorptivity ($mm/sec^{0.5}$ $x10^{-3}$)	Minimize	2.415	4.636
28-day chloride permeability (C)	Minimize	739.30	2475.45
90-day chloride permeability (C)	Minimize	529.85	1467.90
180-day chloride permeability (C)	Minimize	362.40	966.50
Slump value (mm)	Within range	80	210

672

673

5.2. Microstructure of concrete with optimum FA and SF

Scanning electron microscope (SEM) analysis was conducted to examine the microstructure of control and optimized concrete (11.5% SF and 16.3% FA) at 315 days. The SEM images showing the interfacial transition zone (ITZ) of control concrete and optimized concrete are presented in Figure 14 (a) and Figure 14 (b) respectively. The cloud-like morphology is referred to as calcium silicate hydrate (C-S-H). The hexagonal plate-like crystals are referred to as calcium hydroxide ($Ca(OH)_2$). As shown in Figure 14 (a), a few groups of $Ca(OH)_2$ were found abundantly in the cement paste of control concrete. Conversely, a lower amount of $Ca(OH)_2$ was found and more C-S-H was observed in the optimized concrete as shown in Figure 14 (b). This was attributed to the pozzolanic reaction of SF and FA, which consumed the $Ca(OH)_2$ to form the C-S-H strength gel.

Besides, more noticeable pores could be found on the ITZ of control concrete as shown in Figure 14 (a). In contrast, the distribution of cement paste on the ITZ of optimized concrete as in Figure 14 (b) was more uniform, indicating a stronger interlocking bond between the paste and the SiMn slag aggregate. The trace of cement paste filling up the pore on the surface of aggregate was also observed in the optimized concrete. The SEM analysis has shown that the optimized concrete has a more compact microstructure than the control concrete. The findings have confirmed the improved strength and durability of the optimized concrete.

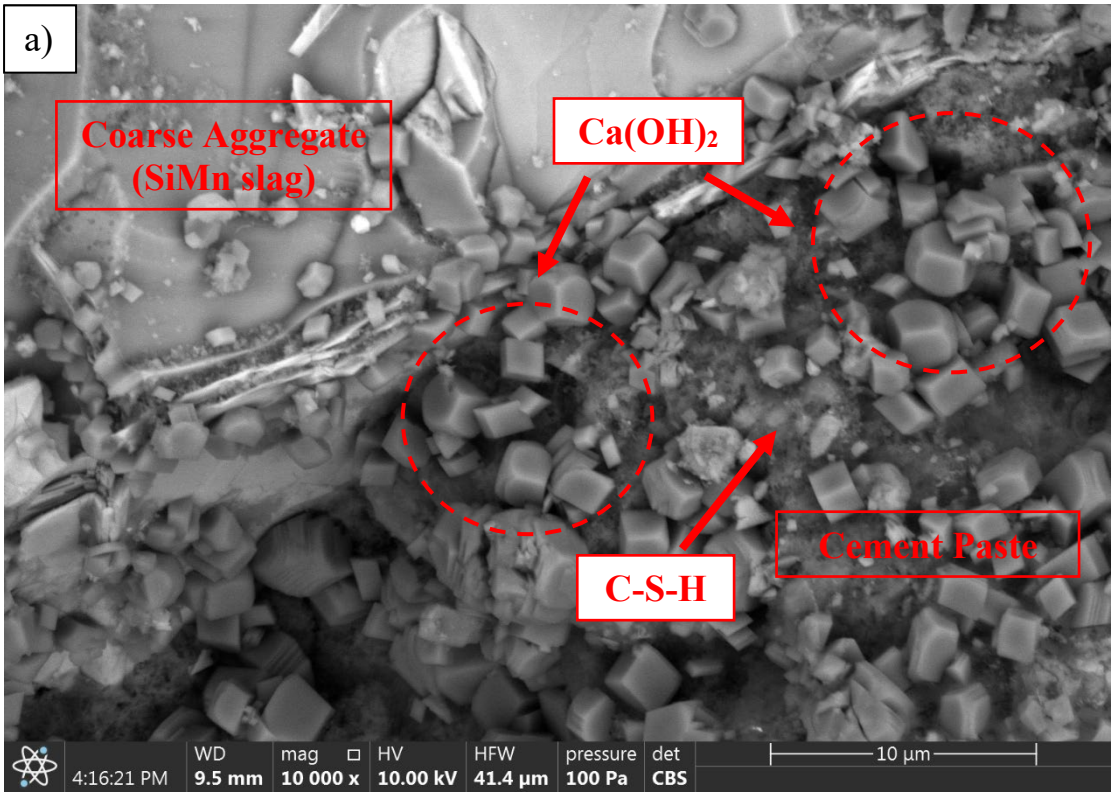

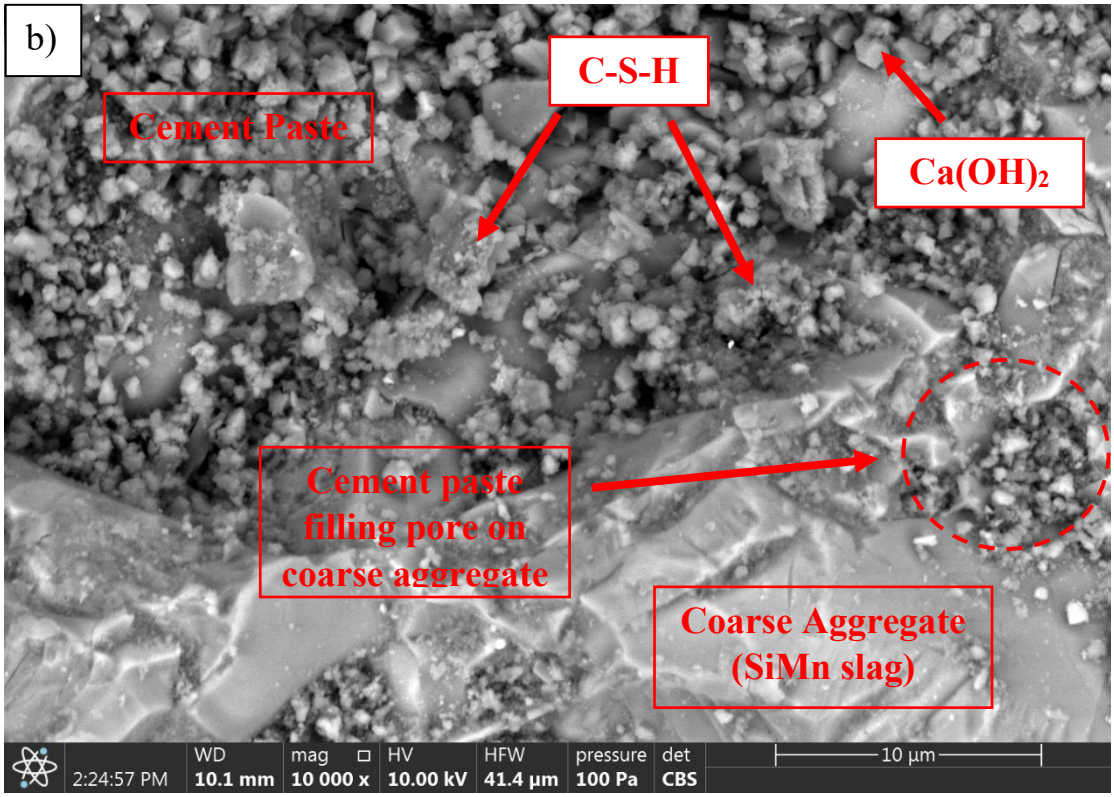

Figure 14: SEM images on interfacial transition zone of (a) control concrete and (b) optimized concrete at 315 days

699 *5.3. Application of prediction model on limestone concrete*

700 The application of the prediction models to concrete produced from the limestone
701 aggregate is presented in this section. Three sets of prediction were made for the 28-
702 day compressive strength targeting 65 MPa, 70 MPa and 75 MPa. The model proposed
703 various predicted outcomes with different combinations of SF/B and FA/B. Selection
704 of the predicted outcomes was based on the use of high SF and FA replacement levels
705 that improved sustainability of concrete. The selected values are shown in Table 12,
706 which are 39% FA and 21.9% SF for test A, 36.6% FA and 17.9% SF for test B, as well
707 as 25.9% FA and 15.7% SF for test C. The 7-day, 28-day and 90-day compressive
708 strengths of SiMn concrete were predicted using the prediction models in Table 6.
709 Using the predicted strength of SiMn slag concrete, the compressive strengths of
710 limestone concrete were obtained from Eqn. (2).

711 Experiments were carried out to validate the predicted compressive strength of SiMn
712 slag and limestone concrete for 7, 28 and 90 days. Concrete specimens were prepared
713 and tested using similar procedures and conditions. Figure 15 presents the test results
714 as well as the comparison with the predicted results. For SiMn slag concrete, the
715 experimental 28-day compressive strength generally achieved the target value for test
716 A, B and C, with an error of 4.6%, 2.6% and 4.6% respectively. Test A concrete had a
717 slightly lower strength than predicted due to its high SF content, which decreased
718 concrete homogeneity. Nonetheless, the issue did not arise in test B and test C. The
719 results further confirmed the accuracy of model in concrete strength prediction.

720 The compressive strength of limestone concrete is higher than that of SiMn slag
721 concrete. But with increasing FA and SF contents, the strength difference was reduced.
722 The improvement in the strength of SiMn slag concrete by FA and SF was more

723 significant than that of limestone concrete. The finding was similar to that of Tang et
724 al. [48], who found a better strength improvement of recycled aggregate concrete made
725 by using blast furnace slag as mineral admixture. Besides, the percentage error for all
726 tests ranged from 0.9% to 5.4%, indicating satisfactory accuracy of Eqn. (2) for the
727 conversion of strength between the SiMn slag and limestone concrete. The use of the
728 RSM models to predict the concrete strength manufactured from limestone aggregate
729 is valid. It is essential that the correlation between the two types of concrete are
730 appropriately established.

731

732 **Table 12: Predicted SF and FA contents at targeted compressive strength**

Test	Targeted 28-day compressive strength	Predicted outcome		
		FA/B	SF/B	Desirability
A	65 MPa	0.390	0.219	1.0
B	70 MPa	0.366	0.179	1.0
C	75 MPa	0.259	0.157	1.0

Slump value was set within 80 mm to 210 mm for Test set A, B and C.

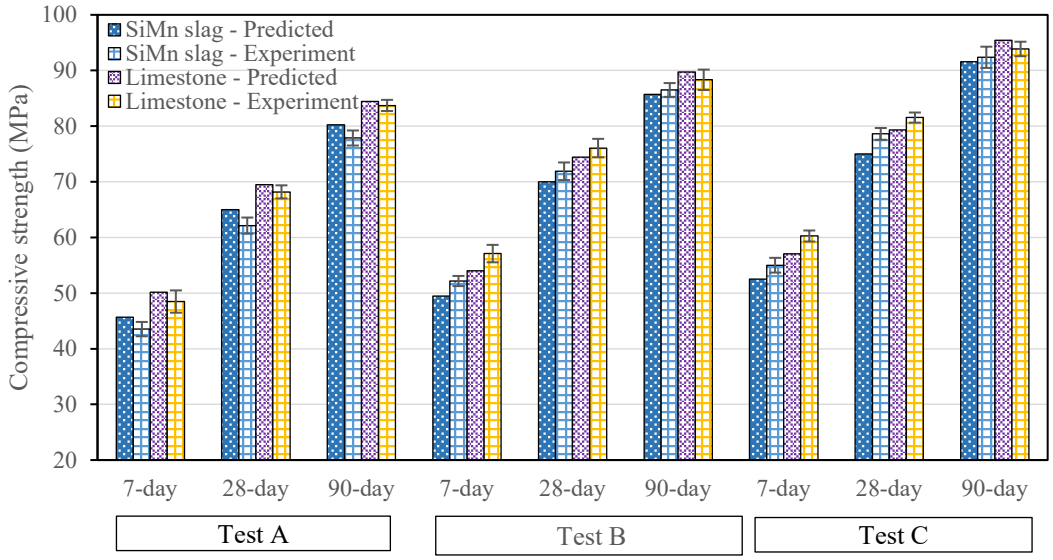

733

734 **Figure 15: Comparison of predicted and experiment compressive strength for**
735 **SiMn slag and limestone concrete**

736

737 *5.4. Further opportunities for optimized FA and SF concrete*

738 The previous section examined and discussed the fundamental properties of concrete.
739 Nonetheless, concrete optimized with FA and SF also has improved advantages in other
740 properties, especially with regard to its practical application. The following further
741 elaborates on the opportunities for the application of optimized FA and SF concrete.

742 *5.4.1. Fracture toughness*

743 The failure of concrete in all states of stress is closely associated with defect due to
744 cracking. Fracture toughness is an important parameter used to describe the mechanism
745 of crack initiation and propagation, especially in the case of brittle materials such as
746 concrete [49]. There are three modes of concrete fracture relating to the three-
747 dimensional failure, namely mode I (K_{Ic}), mode II (K_{IIc}) and mode III (K_{IIIc}). K_{Ic}
748 represents pure tensile loading, K_{IIc} represents in-plane shearing and K_{IIIc} represents
749 anti-plane shearing.

750 Mechanical properties, such as compressive and splitting tensile strength, can directly
751 influence the fracture toughness of concrete. Past research has shown that the use of
752 blends such as FA and SF can increase the strength of concrete and hence its fracture
753 toughness. Golewski [49] found that FA concrete had a lower early-age but higher late-
754 age mode III stress intensity factor (K_{IIIc}), which showed a similar pattern to
755 compressive strength. In addition, Liu et al. [50] showed that the incorporation of 30%
756 SF could increase K_{Ic} by up to 64% because SF improved cement bonding and reduced
757 stress relaxation. Therefore, as the strength of optimized FA and SF concrete has been
758 improved in this study, optimization can also contribute to the improvement of concrete

759 fracture toughness. Nevertheless, further investigation is still required to acquire data
760 to confirm this hypothesis.

761 *5.4.2. Resistance to dynamic load*

762 Dynamic resistance is a key factor in the assessment of material structural performance
763 and safety, especially for concrete, which is a brittle and strain-rate sensitive material
764 [51]. The behavior of concrete under transient dynamic loads, such as earthquake
765 impacts, machine operation and explosion, is different from that of concrete under static
766 loads. Resistance of concrete to dynamic load can be determined by both destructive
767 and non-destructive tests. Destructive test includes drop-weight test, explosive test,
768 projectile impact test and split-Hopskinson bar test [52], whereas the damping test is a
769 non-destructive test [53].

770 As the main interest of most researches is static or quasi-static loading, there are fewer
771 investigations documenting dynamic behaviors of concrete, particularly those
772 optimized with SF and FA. Optimized concrete, which possesses high strength and high
773 durability, is perceived to also exhibit better resistance to dynamic loading. Zhao and
774 Zhang [54] have found that the dynamic tensile strength has increased with SF content
775 due to improved concrete pore structure. Finer property of SF filled the particle gap in
776 cement and thus reduced the porosity. In contrast, Nili and Afroughsabet [51] found
777 that the improvement of impact resistance by SF was not proportional to the increased
778 compressive strength as concrete became more brittle. Nonetheless, FA can be used to
779 increase the ductility of concrete, which may improve its dynamic resistance, but this
780 requires further investigation [55].

781 *5.4.3. Synergy with other additives*

782 The current study focuses on the optimization of ternary cement using FA and SF to
783 maximize the mechanical and durability properties of concrete. Research can be
784 expanded by the introduction of other additives such as ground granulated blast furnace
785 slag (GGBS), metakaolin (MK) and marble waste powder (MWP) to further boost
786 concrete performance. Gesoğlu et al. [56] showed that the addition of GGBS as
787 quaternary cement could reduce the sorptivity and chloride permeability of FA and SF
788 concrete. Slag, such as GGBS, typically contains chemical compositions that are more
789 stable and can thus facilitate better pozzolanic reaction. Dave et al. [57] have
790 demonstrated that MK is better additive than GGBS in terms of strength due to the
791 higher content of silica and alumina for pozzolanic reaction. In addition, Choudhary et
792 al. [58] found that the use of quaternary cement containing FA, SF and MWP at a
793 replacement level of up to 50% could produce concrete with lower permeability than
794 control concrete due to pore refining. In line with the latest research trend towards
795 environmental sustainability, the use of high-volume cement replacement without
796 comprising strength and durability is of best interest. Future study is recommended to
797 consider the synergy of FA and SF concrete with other additives in optimization so as
798 to produce more sustainable concrete.

799

800 **6. Conclusion**

801 This research uses binary and ternary cement blends of SF and FA to enhance the
802 strength and durability of SiMn slag concrete using the Response Surface Method
803 (RSM). Based on the outcomes of the experiment and also the optimization, the
804 following conclusion can be drawn.

1. Concrete compressive and splitting tensile strength showed a similar result pattern. Incorporation of SF up to 15% increased strength at all ages, but a further addition reduced strength. FA incorporation of up to 40% increased 28-day and 90-day strength, but decreased 7-day strength due to slow pozzolanic reaction. For ternary blended concrete, SF compensated for reduced 7-day strength caused by FA and their combined effect further increased strength at 28 and 90 days.
2. For durability, the use of 0–15% SF reduced concrete sorptivity. But, when the SF content was above 15%, the sorptivity increased. Concrete containing 0–40% FA exhibited lower sorptivity than the control. Ternary blended concrete further reduced sorptivity, with FA20SF15 concrete having the largest reduction of 38.1%, 20.9% and 20.3% at 28, 90 and 180 days respectively.
3. Chloride permeability of binary and ternary blended concrete decreased with increasing SF and FA contents. FA40SF30 concrete had the lowest chloride permeability at 28, 90 and 180 days, with a reduction of 70.1%, 63.9% and 62.5% respectively.
4. Using the RSM, prediction models for compressive and splitting tensile strengths at 7, 28 and 90 days were presented as quadratic models. Cubic models were developed for sorptivity at 28, 90 and 180 days, chloride permeability at 180 days and concrete slump. Quartic models were developed for chloride permeability at 28 and 90 days.
5. The prediction models were evaluated as statistically significant based on the two-way ANOVA with significance level below 0.05. Residual errors from lack of fit and pure errors were minimal. The adjusted and predicted R^2 showed that the prediction models were adequate to describe the relationship between variables and responses and were fit for optimization.

6. From optimization, the SF and FA contents with maximum strength and minimum permeability were 11.5% and 16.3% respectively. The 90-day compressive strength, 90-day tensile strength, 180-day sorptivity, 180-day chloride permeability were improved by 10.4%, 18.9%, 24.9% and 44.6% respectively. These properties were also improved by 4.2%, 1.6%, 27.3% and 24% respectively, compared to normal limestone concrete.
7. The SEM analysis confirmed that the optimized concrete exhibited a more compact ITZ and better bonding of cement paste with aggregate than the control.
8. A linear equation was established to correlate the compressive strength between SiMn slag and limestone concrete. The equation used in conjunction with the RSM models predicted the compressive strength of limestone concrete with good accuracy. Further research is recommended to establish correlation of durability between SiMn slag and limestone concrete to be used with RSM models for prediction purpose.

Acknowledgement

The authors would like to thank Curtin Universtiy Malaysia for providing research support and Novakey Developers Sdn. Bhd. for providing research fund.

Reference

[1] Kim, B.-S., S.-B. Jeong, M.-H. Jeong, and J.-W. Ryu, *Upgrading of Manganese from Waste Silicomanganese Slag by a Mechanical Separation Process.* Materials Transactions, 2011. **52**(8): p. 1705-1708.
[2] Oliveira, R.W.H., G. Fernandes, F.C. Sousa, and R.A. Barreto, *Chemical and mineralogical characterization of silicon manganese iron slag as railway ballast.* REM-International Engineering Journal, 2017. **70**(4): p. 385-391.
[3] Frias, M., M.I.S. de Rojas, J. Santamaría, and C. Rodríguez, *Recycling of silicomanganese slag as pozzolanic material in Portland cements: basic and engineering properties.* Cement and Concrete Research, 2006. **36**(3): p. 487-491.
[4] Nath, S. and S. Kumar, *Evaluation of the suitability of ground granulated silico-manganese slag in Portland slag cement.* Construction and Building Materials, 2016. **125**: p. 127-134.

[5] Allahverdi, A. and S. Ahmadnezhad, *Mechanical activation of silicomanganese slag and its influence on the properties of Portland slag cement.* Powder technology, 2014. **251**: p. 41-51.
[6] Navarro, R., E. Zornoza, P. Garcés, I. Sánchez, and E. Alcocel, *Optimization of the alkali activation conditions of ground granulated SiMn slag.* Construction and Building Materials, 2017. **150**: p. 781-791.
[7] Ting, M.Z.Y., K.S. Wong, M.E. Rahman, and M.S. Joo, *Mechanical and durability performance of marine sand and seawater concrete incorporating silicomanganese slag as coarse aggregate.* Construction and Building Materials, 2020. **254**: p. 119195.
[8] Bhanja, S. and B. Sengupta, *Influence of silica fume on the tensile strength of concrete.* Cement and concrete research, 2005. **35**(4): p. 743-747.
[9] Mazloom, M., A. Ramezanianpour, and J. Brooks, *Effect of silica fume on mechanical properties of high-strength concrete.* Cement and Concrete Composites, 2004. **26**(4): p. 347-357.
[10] Song, H.-W., J.-C. Jang, V. Saraswathy, and K.-J. Byun, *An estimation of the diffusivity of silica fume concrete.* Building and Environment, 2007. **42**(3): p. 1358-1367.
[11] Kwan, A. and J. Chen, *Adding fly ash microsphere to improve packing density, flowability and strength of cement paste.* Powder technology, 2013. **234**: p. 19-25.
[12] Ponikiewski, T. and J. Gołaszewski, *The influence of high-calcium fly ash on the properties of fresh and hardened self-compacting concrete and high performance self-compacting concrete.* Journal of cleaner production, 2014. **72**: p. 212-221.
[13] Sumer, M., *Compressive strength and sulfate resistance properties of concretes containing Class F and Class C fly ashes.* Construction and Building Materials, 2012. **34**: p. 531-536.
[14] Radlinski, M. and J. Olek, *Investigation into the synergistic effects in ternary cementitious systems containing portland cement, fly ash and silica fume.* Cement and Concrete Composites, 2012. **34**(4): p. 451-459.
[15] Bagheri, A., H. Zanganeh, H. Alizadeh, M. Shakerinia, and M.A.S. Marian, *Comparing the performance of fine fly ash and silica fume in enhancing the properties of concretes containing fly ash.* Construction and building materials, 2013. **47**: p. 1402-1408.
[16] Erdem, T.K. and Ö. Kırca, *Use of binary and ternary blends in high strength concrete.* Construction and Building Materials, 2008. **22**(7): p. 1477-1483.
[17] Thomas, M., M. Shehata, S. Shashiprakash, D. Hopkins, and K. Cail, *Use of ternary cementitious systems containing silica fume and fly ash in concrete.* Cement and concrete research, 1999. **29**(8): p. 1207-1214.
[18] Nehdi, M. and J. Summer, *Optimization of ternary cementitious mortar blends using factorial experimental plans.* Materials and structures, 2002. **35**(8): p. 495-503.
[19] Muthukumar, M., D. Mohan, and M. Rajendran, *Optimization of mix proportions of mineral aggregates using Box Behnken design of experiments.* Cement and Concrete Composites, 2003. **25**(7): p. 751-758.
[20] Güneyisi, E., M. Gesoğlu, Z. Algın, and K. Mermerdaş, *Optimization of concrete mixture with hybrid blends of metakaolin and fly ash using response surface method.* Composites Part B: Engineering, 2014. **60**: p. 707-715.
[21] Rezaifar, O., M. Hasanzadeh, and M. Gholhaki, *Concrete made with hybrid blends of crumb rubber and metakaolin: optimization using response surface method.* Construction and building materials, 2016. **123**: p. 59-68.
[22] *ASTM C150, Standard specification of Portland cement*. 2012, American Society for Testing and Materials: West Conshohocken, PA.
[23] Whitcomb, P.J. and M.J. Anderson, *RSM simplified: optimizing processes using response surface methods for design of experiments*. 2004: CRC press.
[24] Design-Expert, *Software for design of experiments.* 2018, Stat-Ease Corporation: Minneapolis, USA.

[25] Aldahdooh, M., N.M. Bunnori, and M.M. Johari, *Evaluation of ultra-high-performance-fiber reinforced concrete binder content using the response surface method.* Materials & Design (1980-2015), 2013. **52**: p. 957-965.
[26] Tripathi, D., R. Kumar, P. Mehta, and A. Singh, *Silica fume mixed concrete in acidic environment.* Materials Today: Proceedings, 2020.
[27] Ahmad, O.A., *Production of High-Performance Silica Fume Concrete.* American journal of applied sciences, 2017. **14**(11): p. 1031.1038.
[28] DeRousseau, M., J. Kasprzyk, and W. Srubar III, *Computational design optimization of concrete mixtures: A review.* Cement and Concrete Research, 2018. **109**: p. 42-53.
[29] *ASTM C192, Standard practice for making and curing concrete test specimens in the laboratory*. 2012, American Society for Testing and Materials: West Conshohocken, PA.
[30] *ASTM C143, Standard test method for slump of hydraulic-cement concrete*. 2015, American Society for Testing and Materials: West Conshohocken, PA.
[31] *ASTM C39, Standard test method for compressive strength of cylinderical concrete specimens*. 2012, American Society for Testing and Materials: West Conshohocken, PA.
[32] *ASTM C496, Standard test method for splitting tensile strength of cylindrical concrete specimens*. 2012, American Society for Testing and Materials: West Conshohocken, PA.
[33] *ASTM C1585, Standard test method for measurement of rate of absorption of water by hydraulic-cement concrete*. 2012, American Society for Testing and Materials: West Conshohocken, PA.
[34] *ASTM C1202, Standard test method for elecrical indication of concrete's ability to resist chloride ion penetration*. 2012, American Society for Testing and Materials: West Conshohocken, PA.
[35] *ACI 304.2R-96, ACI Committee 304: Placing concrete by pumping methods*. 1996, American Concrete Institute: Farmington Hills, MI.
[36] Kondraivendhan, B. and B. Bhattacharjee, *Flow behavior and strength for fly ash blended cement paste and mortar.* International Journal of Sustainable Built Environment, 2015. **4**(2): p. 270-277.
[37] Alaka, H.A. and L.O. Oyedele, *High volume fly ash concrete: The practical impact of using superabundant dose of high range water reducer.* Journal of Building Engineering, 2016. **8**: p. 81-90.
[38] Yazici, Ş. and H.Ş. Arel, *Effects of fly ash fineness on the mechanical properties of concrete.* Sadhana, 2012. **37**(3): p. 389-403.
[39] Dave, N., A.K. Misra, A. Srivastava, A.K. Sharma, and S.K. Kaushik, *Study on quaternary concrete micro-structure, strength, durability considering the influence of multi-factors.* Construction and Building Materials, 2017. **139**: p. 447-457.
[40] Neithalath, N. and J. Jain, *Relating rapid chloride transport parameters of concretes to microstructural features extracted from electrical impedance.* Cement and Concrete Research, 2010. **40**(7): p. 1041-1051.
[41] Kılıç, A., C. Atiş, A. Teymen, O. Karahan, F. Özcan, C. Bilim, and M. Özdemir, *The influence of aggregate type on the strength and abrasion resistance of high strength concrete.* Cement and Concrete Composites, 2008. **30**(4): p. 290-296.
[42] Bayramov, F., C. Taşdemir, and M. Taşdemir, *Optimisation of steel fibre reinforced concretes by means of statistical response surface method.* Cement and concrete composites, 2004. **26**(6): p. 665-675.
[43] Sonebi, M., *Medium strength self-compacting concrete containing fly ash: Modelling using factorial experimental plans.* Cement and Concrete research, 2004. **34**(7): p. 1199-1208.
[44] Lotfy, A., K.M. Hossain, and M. Lachemi, *Application of statistical models in proportioning lightweight self-consolidating concrete with expanded clay aggregates.* Construction and Building Materials, 2014. **65**: p. 450-469.

[45] Noordin, M.Y., V. Venkatesh, S. Sharif, S. Elting, and A. Abdullah, *Application of response surface methodology in describing the performance of coated carbide tools when turning AISI 1045 steel.* Journal of materials processing technology, 2004. **145**(1): p. 46-58.
[46] EN, B., *12350-2,"Testing fresh concrete-Part 2: Slump test".* European Committee for Standardization, 2009.
[47] Myers, R.H., D.C. Montgomery, and C.M. Anderson-Cook, *Response surface methodology: process and product optimization using designed experiments*. 2016: John Wiley & Sons.
[48] Tang, Z., Y. Hu, V.W. Tam, and W. Li, *Uniaxial compressive behaviors of fly ash/slag-based geopolymeric concrete with recycled aggregates.* Cement and Concrete Composites, 2019. **104**: p. 103375.
[49] Golewski, G.L., *Effect of curing time on the fracture toughness of fly ash concrete composites.* Composite Structures, 2018. **185**: p. 105-112.
[50] Liu, Y., C. Shi, Z. Zhang, N. Li, and D. Shi, *Mechanical and fracture properties of ultra-high performance geopolymer concrete: Effects of steel fiber and silica fume.* Cement and Concrete Composites, 2020: p. 103665.
[51] Nili, M. and V. Afroughsabet, *Combined effect of silica fume and steel fibers on the impact resistance and mechanical properties of concrete.* International journal of impact engineering, 2010. **37**(8): p. 879-886.
[52] Song, P., J. Wu, S. Hwang, and B. Sheu, *Assessment of statistical variations in impact resistance of high-strength concrete and high-strength steel fiber-reinforced concrete.* Cement and Concrete Research, 2005. **35**(2): p. 393-399.
[53] Noushini, A., B. Samali, and K. Vessalas, *Effect of polyvinyl alcohol (PVA) fibre on dynamic and material properties of fibre reinforced concrete.* Construction and Building Materials, 2013. **49**: p. 374-383.
[54] Zhao, S. and Q. Zhang, *Effect of Silica Fume in Concrete on Mechanical Properties and Dynamic Behaviors under Impact Loading.* Materials, 2019. **12**(19): p. 3263.
[55] Ali, B., L.A. Qureshi, S.H.A. Shah, S.U. Rehman, I. Hussain, and M. Iqbal, *A step towards durable, ductile and sustainable concrete: Simultaneous incorporation of recycled aggregates, glass fiber and fly ash.* Construction and Building Materials, 2020. **251**: p. 118980.
[56] Gesoğlu, M., E. Güneyisi, and E. Özbay, *Properties of self-compacting concretes made with binary, ternary, and quaternary cementitious blends of fly ash, blast furnace slag, and silica fume.* Construction and Building Materials, 2009. **23**(5): p. 1847-1854.
[57] Dave, N., A.K. Misra, A. Srivastava, A.K. Sharma, and S.K. Kaushik, *Green quaternary concrete composites: Characterization and evaluation of the mechanical properties.* Structural Concrete, 2018. **19**(5): p. 1280-1289.
[58] Choudhary, R., R. Gupta, R. Nagar, and A. Jain, *Sorptivity characteristics of high strength self-consolidating concrete produced by marble waste powder, fly ash, and micro silica.* Materials Today: Proceedings, 2020.